

Tetrahydronaphththyridine and Dihydronaphththyridinone Ethers As Positive Allosteric Modulators of the Metabotropic Glutamate Receptor 5 (mGlu₅)

Mark Turlington,^{†,‡,§} Chrysa Malosh,^{†,‡,§} Jon Jacobs,^{†,‡,§} Jason T. Manka,^{†,‡,§} Meredith J. Noetzel,^{†,‡} Paige N. Vinson,^{†,‡} Satyawar Jadhav,^{†,‡} Elizabeth J. Herman,^{†,‡} Hilde Lavreysen,[#] Claire Mackie,[∇] José M. Bartolomé-Nebreda,[○] Susana Conde-Ceide,[○] M. Luz Martín-Martín,[○] Han Min Tong,[○] Silvia López,[○] Gregor J. MacDonald,[#] Thomas Steckler,[#] J. Scott Daniels,^{†,‡,§} C. David Weaver,^{†,‡} Colleen M. Niswender,^{†,‡,§} Carrie K. Jones,^{†,‡,§} P. Jeffrey Conn,^{†,‡,§} Craig W. Lindsley,^{†,‡,§,||} and Shaun R. Stauffer^{*,†,‡,§,||}

[†]Department of Pharmacology, Vanderbilt University Medical Center, Nashville, Tennessee 37232, United States

[‡]Vanderbilt Center for Neuroscience Drug Discovery, Vanderbilt University Medical Center, 1205 Light Hall, Nashville, Tennessee 37232-0697, United States

[§]Vanderbilt Specialized Chemistry Center for Probe Development (MLPCN), Nashville, Tennessee 37232, United States

^{||}Department of Chemistry, Vanderbilt University, Nashville, Tennessee 37232, United States

[⊥]Vanderbilt Institute of Chemical Biology, Vanderbilt University, Nashville, Tennessee 37232, United States

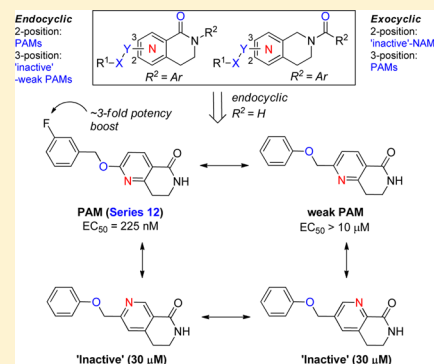
[#]Neuroscience, Janssen Research and Development, Turnhoutseweg 30, B-2340, Beerse, Belgium

[∇]Discovery Sciences ADME/Tox, Janssen Research and Development, Turnhoutseweg 30, B-2340, Beerse, Belgium

[○]Neuroscience Medicinal Chemistry, Janssen Research and Development, Jarama 75, 45007 Toledo, Spain

Supporting Information

ABSTRACT: Positive allosteric modulators (PAMs) of metabotropic glutamate receptor 5 (mGlu₅) represent a promising therapeutic strategy for the treatment of schizophrenia. Starting from an acetylene-based lead from high throughput screening, an evolved bicyclic dihydronaphththyridinone was identified. We describe further refinements leading to both dihydronaphththyridinone and tetrahydronaphththyridine mGlu₅ PAMs containing an alkoxy-based linkage as an acetylene replacement. Exploration of several structural features including western pyridine ring isomers, positional amides, linker connectivity/position, and combinations thereof, reveal that these bicyclic modulators generally exhibit steep SAR and within specific subseries display a propensity for pharmacological mode switching at mGlu₅ as well as antagonist activity at mGlu₃. Structure–activity relationships within a dihydronaphththyridinone subseries uncovered 12c (VU0405372), a selective mGlu₅ PAM with good in vitro potency, low glutamate fold-shift, acceptable DMPK properties, and in vivo efficacy in an amphetamine-based model of psychosis.



INTRODUCTION

Schizophrenia is a complex mental illness characterized by positive (hallucinations, paranoia, disorganized behavior) and negative symptoms (social withdrawal, anhedonia, flat affect) as well as cognitive dysfunction (deficits in attention, learning, and memory).^{1–4} Current treatments, including typical and second-generation atypical antipsychotics, are based largely upon the dopaminergic hypothesis of schizophrenia, which targets overactivation of subcortical dopamine D₂ receptors.⁵ Both classes treat the positive symptoms; however, neither class of antipsychotics has made a substantial impact on the negative and cognitive symptoms.^{1–4} After several decades of clinical use, a significant understanding of the risks and side effect

profiles that plague both classes of antipsychotics has been gained. These include extrapyramidal side effects, sexual dysfunction, weight gain (metabolic syndrome), agranulocytosis, increased cardiac risk, and poor patient compliance.^{3,6,7}

The development of positive allosteric modulators (PAMs) of metabotropic glutamate receptor 5 (mGlu₅)⁸ as a novel approach to test the glutamate or *N*-methyl-D-aspartate (NMDA) receptor hypofunction hypothesis of schizophrenia^{9–14} has provided preclinical evidence for therapeutic potential in multiple psychosis and cognitive animal mod-

Received: February 18, 2014

Published: June 10, 2014

els,^{10,12–14} and, for more than a decade, industry and academic drug discovery groups have been in pursuit of brain penetrant small molecule mGlu₅ potentiators.^{15,16} A testament to the success of the field has been the identification of over eight reported chemotypes^{15,16} with in vivo efficacy in preclinical models, beginning with 3-cyano-*N*-(1,3-diphenyl-1*H*-pyrazol-5-yl)benzamide (CDPPB, **1**),¹⁷ piperidiny 1,2,4-oxadiazoles from Addex (ADX-47273, **2**),^{18,19} and subsequently acetylenes *N*-methyl-5-(phenylethynyl)pyrimidin-2-amine (MPPA, **3**),²⁰ VU0360172 (**4**),²¹ LSN2463359 (**8**),^{22,23} piperazines VU0364289 (**5**)²⁴ and 1-(4-(2-chloro-4-fluorophenyl)-piperazin-1-yl)-2-(pyridin-4-ylmethoxy)ethanone (CPPZ, **6**),²⁵ ether VU0404251 (**7**),²⁶ and triazole LSN2814617 from Lilly (**9**).²³ However, recent findings from Merck-Addex and at the Vanderbilt Center for Neuroscience Drug Discovery (VCNDD) have unveiled a target mediated CNS adverse-effect (AE) liability, driven by excessive glutamate fold potentiation²⁷ or allosteric agonism,^{28,29} respectively; suggesting that PAMs with lower functional cooperativity with glutamate (e.g., glutamate fold-shift or potentiation) and devoid of allosteric agonism may be preferred for improved therapeutic index.³⁰ More recently, we disclosed a phenoxy-based ether dihydrothiazolopyridone series,³¹ with the representative in vivo tool compound VU0408899 (**10**) (Figure 1). Ether **10**

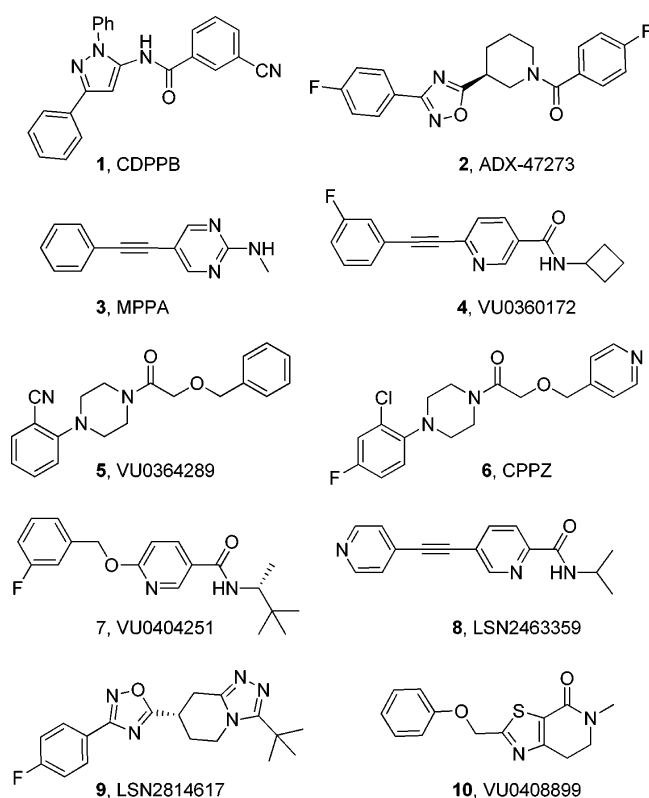


Figure 1. mGlu₅ receptor PAMs with reported efficacy in preclinical models of schizophrenia and cognition.^{17–26,31}

represents, in part, efforts to constrain amides of type **7**; however, due to inherent instability in acidic media (20% HP- β -CD in water, pH = 4) leading to the corresponding 2-hydroxy-dihydrothiazolopyridone fragment, full exploration of the analogous system containing a benzyloxy ether linkage was not possible. Limited in vitro structure–activity relationships (SAR) suggested a preference for the phenoxy-based linker

within the dihydrothiazolopyridones (two examples tested);³¹ however, this trend was not found within monocyclic nicotinamides of type **7**.²⁶ Thus, it was unknown if alteration of the linker moiety within the context of a bicyclic system to more closely mimic **7** (e.g., dihydronaphthridinone core structures **12**–**17**, Figure 2), would be productive for mGlu₅

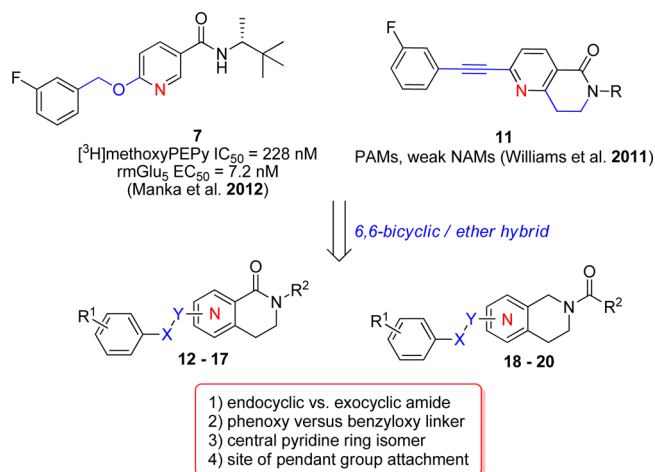
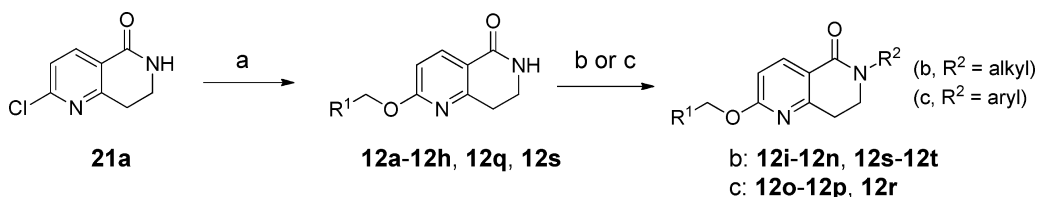
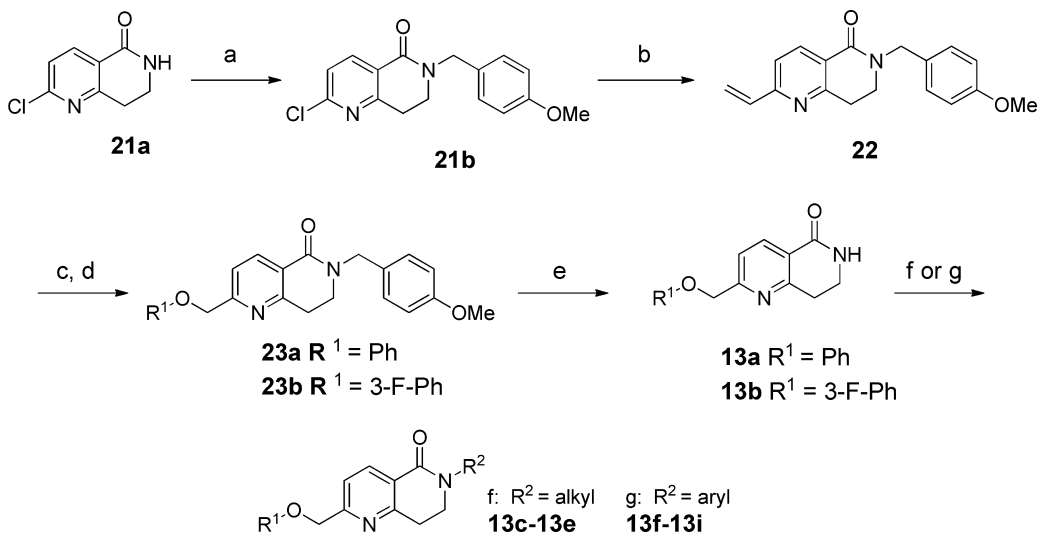


Figure 2. Evolution of tetrahydronaphthridine and dihydronaphthridinone ether based mGlu₅ allosteric modulators (**12**–**20**) from nicotinamide **7**²⁶ and acetylenic modulator scaffold **11**.³²

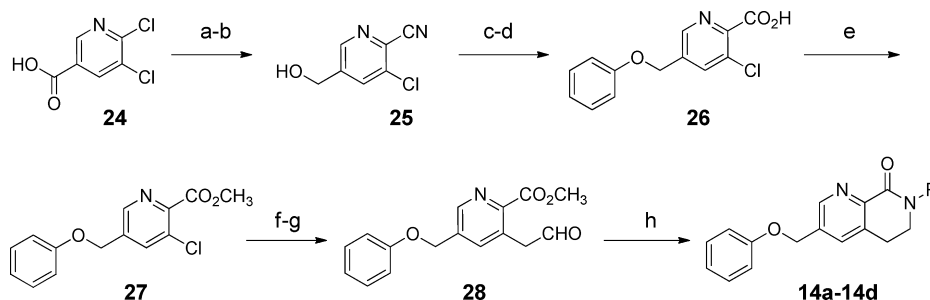
receptor potentiation. Prior studies within a dihydronaphthridinone class utilizing an acetylene-based linker, initially identified from an HTS screen, led to PAMs with submicromolar potency,³² including dihydronaphthridinones **11**, suggested that linkers employing either $-\text{CH}_2\text{O}-$ or $-\text{OCH}_2-$ might be successful as an acetylene replacement. Interestingly, evidence of subtle “molecular switches”^{15,33} within acetylenic dihydronaphthridinones **11** via simple amide congeners led to fundamental changes in the mode of pharmacology (e.g., from PAMs to negative allosteric modulators or NAMs).¹⁵ The pursuit of ethers **12**–**20** were undertaken as part of a larger comprehensive study aimed to target four key structure–activity relationships: (1) endocyclic versus exocyclic amide, (2) phenoxy versus benzyloxy linker, (3) central ring pyridine isomers, and (4) site of the pendant group attachment to central heterocycle. It was unclear at the outset if ethers **12**–**20** would exhibit subtle changes in the mode of pharmacology similar to **11**³² and other chemotypes^{30,34,35} or would maintain a higher fidelity for potentiation similar to CDPPB (**1**),^{17,36,37} *N*-[5-chloro-2-[(1,3-dioxoisindolin-2-yl)methyl]phenyl]-2-hydroxybenzamide (CPPHA),^{38–40} piperazines (**5**–**6**),^{24,25,41} and glycine sulfonamide (ML332)⁴² based mGlu₅ PAMs. Herein we describe the synthesis and pharmacological profile of a series of tetrahydronaphthridine and dihydronaphthridinone ethers (**12**–**20**) as positive allosteric modulators of mGlu₅.^{43–45} Low cooperativity PAM **12c** (VU0405372) was ultimately identified and found to demonstrate a suitable balance of in vitro and in vivo properties for proof-of-concept studies in an amphetamine hyperlocomotor challenge model. In contrast to previously reported and related monocyclic ether series,^{26,31} these bicyclic modulator scaffolds were overall found to exhibit narrow SAR, low efficacy, and have a higher propensity for pharmacological “mode switching”¹⁵ upon chemical modification, demonstrating an SAR profile reminiscent of related acetylenic PAMs.³²

Scheme 1. Synthesis of Alkoxy Dihydro-1,6-naphthyridinone Lactams 12^a

^aReagents and conditions: (a) **21a**, R¹CH₂OH, KO^t-Bu, DMF, 100 °C, 4–16 h, 23–63%; (b) lactam, R²CH₂Br or R²CH₂Cl, KO^t-Bu, DMF, 60 °C, 2–4 h, 40–75%; (c) lactam, CuI (0.2 equiv), Ar/HetBr, *N,N*-dimethylethylenediamine, K₂CO₃, toluene, 120 °C, 18 h, 35–59%.

Scheme 2. Synthesis of Alkoxyethyl Dihydro-1,6-naphthyridinone Lactams 13^a

^aReagents and conditions: (a) **21a**, PMBCl, KO^t-Bu, DMF, 60 °C, 2 h, 66%; (b) vinyl potassium trifluoroborate, Cs₂CO₃, Pd(PPh₃)₄, EtOH, 80 °C, 2 h, 74%; (c) O₃, CH₂Cl₂:MeOH, −78 °C, 40 min, NaBH₄, 0 °C; (d) R¹OH, DIAD, PPh₃, THF, 0 °C, 16 h, 35–40% (over two steps); (e) CAN, CH₃CN:H₂O, rt, 50 min, 60–65%; (f) **13a–b**, R²CH₂Br or R²CH₂Cl, KO^t-Bu, DMF, 60 °C, 2–4 h, 44–68%; (g) **13a–b**, CuI (0.2 equiv), Ar/HetBr, *N,N*-dimethylethylenediamine, K₂CO₃, toluene, 120 °C, 18 h, 25–89%.

Scheme 3. Synthesis of Phenoxyethyl Dihydro-1,7-naphthyridinones Lactams 14^a

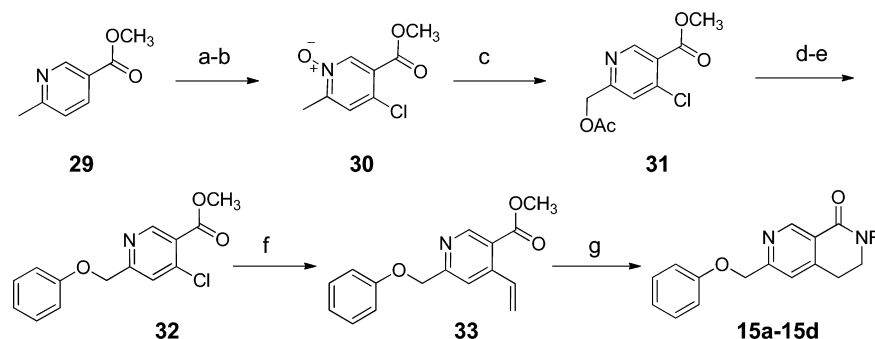
^aReagents and conditions: (a) **24**, BH₃, THF, 0 °C, 16 h, 68%; (b) Zn(CN)₂, Cs₂CO₃, Pd(PPh₃)₄, DMF, 100 °C, 3 h, 56%; (c) DBAB, phenol, PPh₃, THF, 0–120 °C, 40 min, 80%; (d) NaOH, 115 °C, 3 h, quant; (e) CH₃I, K₂CO₃, DMF, rt, 16 h, 73%; (f) Bu₃Sn(allyl), Pd(PPh₃)₄, toluene, 125 °C, 16 h, 56%; (g) NaIO₄, OsO₄, THF, 0 °C–rt, 2 h, 74%; (h) RNH₂, THF-MeOH, NaBH(OAc)₃, rt, 16 h, 15–25%.

RESULTS AND DISCUSSION

Chemistry. To prepare bicyclic analogues that most closely mimic the structural features found in **11**, we initially prepared a series of dihydro-1,6-naphthyridin-5(6*H*)-ones (**12a–12t**, Scheme 1). Starting from known compound 2-chloro-7,8-dihydro-1,6-naphthyridin-5(6*H*)-one (**21a**, Supporting Information), substitution under basic conditions in the presence of various alcohols with heating afforded **12a–12h**, **12q**, and **12s** in low to moderate yield. A subset was treated with alkylating agents under basic conditions, or with various aryl and

heteroaryl halides using a copper iodide–diamine ligand protocol to effect a modified Ullman lactam cross-coupling to give the respective alkyl (**12i–12n**, **12s–12t**) and *N*-aryl (**12o–12p**, **12r**) lactam products.

Evaluation of the alternate ether linkage based upon an aryloxy methyl dihydronaphthyridinone, series **13**, began synthetically from **21a** as shown in Scheme 2. Protection with *para*-methoxybenzyl chloride (PMBCl) afforded **21b** in good yield. Suzuki–Miyaura coupling under Molander's conditions using vinyl potassium trifluoroborate salt gave

Scheme 4. Synthesis of Phenoxyethyl-dihydro-2,7-naphthyridinones 15^a

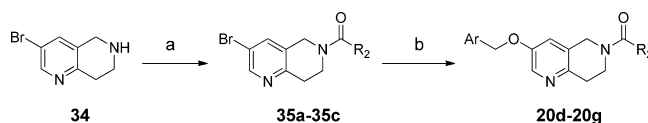
^aReagents and conditions: (a) 29, POCl₃, 16 h, 95 °C, 68%; (b) cat. CH₃ReO₃, H₂O₂, CH₂Cl₂, 16 h, rt, quant; (c) Ac₂O, 120 °C, 45 min, 11%; (d) K₂CO₃, MeOH, rt, 15 min, 92%; (e) DBAB, phenol, PPh₃, THF, 60 °C, 16 h, 73%; (f) Bu₃(vinyl)Sn, Pd(PPh₃)₄, toluene–dioxane, 90 °C, 16 h, 76%; (g) amine/ammonia in THF or MeOH, sealed tube, 100 °C, 16 h, 39–93%.

vinyl dihydronaphthyridinone intermediate 22. Subsequent ozonolysis and reductive work-up gave intermediate alcohol 23. Mitsunobu alkylation in the presence of either phenol or 3-fluorophenol provided 23a–23b in 35–40% yield over two steps from 22. Removal of the PMB protecting group using cerium ammonium nitrate proceeded smoothly to give 13a–13b. Remaining analogues 13c–13i were prepared similarly as demonstrated for series 12, using alkylating conditions or copper-based arylation conditions to give alkyl and *N*-aryl lactam products 13c–13e and 13f–13i, respectively.

Within a third class of lactams 14 (Scheme 3), a benzyloxy linkage was retained and an alternate dihydro-1,7-naphthyridinone ring system was explored, placing the pyridine nitrogen at the position ortho to the lactam amide. Synthesis of series 14 began with borane reduction of 5,6-dichloronicotinic acid 24 and subsequent cyanation using Pd(0) catalysis to give 25 in moderate yield. Treatment of 25 under Mitsunobu conditions using phenol and di-*tert*-butyl azodicarboxylate (DBAB), followed by hydrolysis and ester formation, afforded chloroester 27. Allylation of 27 using Stille conditions with allyl tributyltin, followed by osmium tetroxide–sodium periodate mediated cleavage, provided key aldehyde intermediate 28 in good yield for the two steps. At this stage, installation of the lactam could be accomplished using a variety of amines in a one-pot two-step reductive alkylation, ring-cyclization reaction using sodium triacetoxyborohydride in THF–MeOH to provide examples 14a–14d in low to moderate yield.

Synthesis of phenoxyethyl-dihydro-2,7-naphthyridinones 15 was accomplished using a seven-step sequence from methyl-6-methylnicotinate (29) as shown in Scheme 4 and represented the fourth class of dihydronaphthyridinones investigated. Chlorination followed by pyridine *N*-oxide formation using catalytic methyltrioxorhenium(VII) in the presence of hydrogen peroxide gave intermediate 30. Polonovski rearrangement to give acetate 31 followed in low yield. Hydrolysis and subsequent Mitsunobu alkylation provided ether 32 in good yield. Installation of the vinyl moiety using Stille conditions provided key pyridine intermediate 33 in good yield. Vinylpyridine 33 smoothly underwent one-pot Michael addition and lactam cyclization using ammonia or several alkyl and aryl amines to give 15a–15d in moderate to excellent yield.

Alternative tetrahydronaphthyridines wherein the ether linkage is appended at the 3-position as a benzyloxy with an exocyclic amide were achieved according to Scheme 5. Starting bromide 34 was treated with HATU coupling conditions to

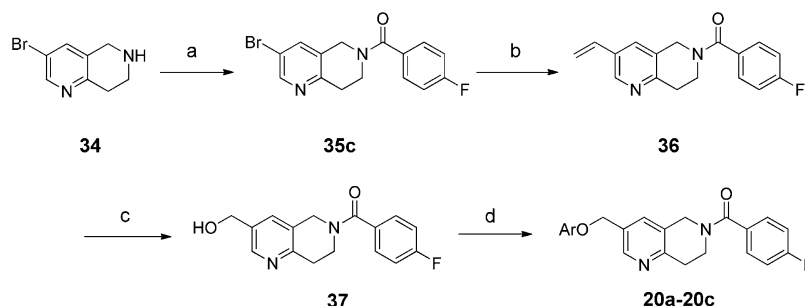
Scheme 5. Synthesis of 3-Benzyloxy-tetrahydro-1,6-naphthyridine Amides 20d–20g^a

^aReagents and conditions: (a) 34, HATU, DIPEA, DMF, rt, 16 h, 60–90%; (b) 35, ArCH₂OH, Cs₂CO₃, 1,10-Phen, CuI, toluene, 110 °C, 4 h, 20–35%.

give amides 35a–35c. Ullman-based etherification using CuI and 1,10-phenanthroline in toluene with heat afforded targets 20d–20g. The related aryloxymethyl targets retaining a similar substitution pattern and acyl-tetrahydronaphthyridine were prepared according to Scheme 6. Initial introduction of amide provided intermediate 35c in 96% yield. Introduction of 4-fluoro-benzamide provided intermediate 35c, followed by Stille cross-coupling to give vinyl 36. Subsequent ozonolysis and reductive work-up gave alcohol 37, which was elaborated via Mitsunobu alkylation to provide 20a–20c in low to moderate yields.

In Vitro Pharmacology. As reported previously,³⁰ compounds were profiled in a rat mGlu₅ low receptor expression cell line using a “triple add” protocol allowing for detection of agonism as well as positive and negative allosteric modulation simultaneously.^{21,46} Importantly, we have shown that detection of allosteric agonism observed using the low receptor expressing cell line correlates with functional response observed in native systems and modulators with an *allosteric agonist* profile have been shown to be associated with epileptiform activity and behavioral convulsions in rodents.^{28–30} In contrast, an allosteric modulator devoid of agonism in these low-expressing mGlu₅ cells was found not to display a seizure liability *in vivo*.²⁸ Thus, this recombinant mGlu₅ cell line in conjunction with the “triple add” protocol provided an important initial *in vitro* assessment of both agonist and potentiation activity at mGlu₅, which could be utilized to prioritize analogues for further progression.

Dihydronaphthyridinones. SAR are shown in Tables 1–4 (12–15, 20) and Figures 4–6 (16–19) and summarize *in vitro* potency optimization efforts from 10 distinct subseries. Initial efforts within Tables 1–2 were focused on further expanding our previously utilized pharmacophore noted within several chemotypes, including acetylene 4,²¹ ethers 7 and 10,^{26,31} which retain a pyridyl nitrogen and an amide oxygen as

Scheme 6. Synthesis of 3-Aryloxymethyl-tetrahydro-1,6-naphthyridine Amides 20a–20c^a

^aReagents and conditions: (a) **34**, 4-fluorobenzoic acid, HATU, DIPEA, DMF, rt, 16 h, 96%; (b) Bu₃(vinyl)Sn, Pd(PPh₃)₄, toluene, 120 °C, 1 h, 82%; (c) O₃, CH₂Cl₂:MeOH, –78 °C, 30 min, NaBH₄, 0 °C; (d) R'OH, DIAD, polystyrene–PPh₃, THF, rt, 16 h, 25–40% (over two steps).

potential hydrogen bond accepting groups in an optimal spatial arrangement as illustrated in Figure 3. As can be seen in Table

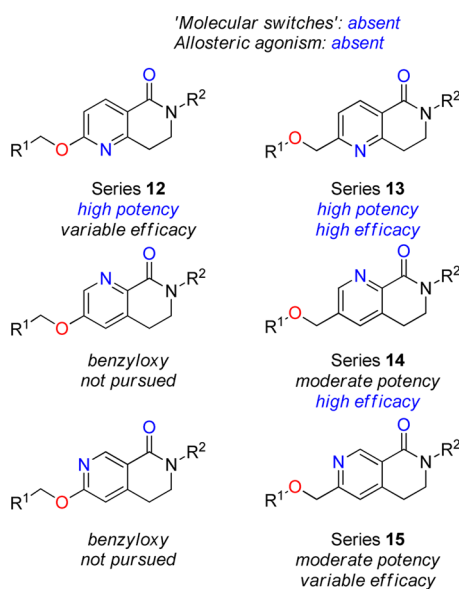


Figure 3. Heterocycle, amide, linker pharmacophore relationships, and relative profile for “endocyclic” series 12–15 dihydronaphthyridinones and hypothetical benzyloxy lactam core regioisomers of 14–15.

1, in the case of 2-benzyloxy derivatives, half of the analogues were active as mGlu₅ PAMs. Among actives, the parent lactams (R = H, **12a–12h**, **12q**) showed a range of potency from 62 to 1171 nM with low to moderate maximal efficacy (glutamate max 43–68%). Notably, no evidence for allosteric agonism was observed for actives in the series. SAR on the R¹ group demonstrated toleration for meta-substituted fluorine and chlorine congeners **12c** and **12e**, respectively, representing two of the more interesting actives from this subseries on the basis of overall potency and efficacy (EC₅₀ < 250 nM, Glu max >40%). *n*-Butyloxy derivatives **12q** and **12r**, reminiscent of a previously disclosed non-MPEP ether PAM, were not successful.⁴⁷ The 2 and 3-pyridyl congeners **12g** and **12h** were also not tolerated at R¹. Additionally, eastern alkyl derivatives **12i–12n** containing linear, branched, cyclic, phenyl, and heterocyclic systems were either inactive (a <10% increase in the baseline EC₂₀ glutamate fluorescence response in calcium assays at the highest concentration tested of 30 μM is defined as “inactive”) or had moderate potency and low efficacy (EC₅₀ > 300 nM, PAM Glu max <40%, **12l–12n**, **12s–12t**). *N*-Aryl

congeners **12o** and **12p** demonstrated comparable potency below 250 nM, with **12p** slightly more efficacious (Glu max 50% vs 38%). Both the western fluoro and the eastern amide *N*-aryl SAR parallel the recently reported thiazolyl core structure system;³¹ however, interestingly, *N*-alkyl derivatives were significantly better tolerated in the thiazolyl ring system.

We next turned to the alternate 2-phenoxy derivatives shown in Table 2. Studies by AstraZeneca Pharmaceuticals⁴⁸ and within the dihydrothiazolopyridone series **10**³¹ have demonstrated successful utilization of the both benzyloxy- and phenoxy-methyl-based spacers as replacements for the acetylene moiety, with varied potency depending on the nature of the heterocycle scaffold.^{26,31,48–50} Interestingly, in contrast to the unsubstituted benzyloxy lactams **12a–12b**, alkoxy-methyl-dihydronaphthyridinones **13a–13b** were weak PAMs (a weak PAM results in a response that is greater than a 10% increase compared to the submaximal glutamate addition (EC₂₀) but does not potentiate the overall glutamate EC₂₀ response by at least 2-fold). Similarly, *N*-alkyl derivatives were not productive as PAMs, leading to compounds categorized as weak or inactive (**13c–13e**, **13i**). Direct *N*-aryl derivatives were more beneficial, with the western 3-fluorophenyl congener **13g** bearing an *N*-4-fluoro-phenyl proving to be potent (EC₅₀ = 97 nM) and efficacious (Glu max = 72%); the 2-pyridyl derivative **13h** was 5-fold less active (EC₅₀ = 595 nM) and less efficacious. Fortunately, introduction of a 3-fluoro moiety on the distal phenyl consistently boosted potency (~2–3-fold) and proved transferrable among the subseries (e.g., **13f** vs **13g**). The potency for **13g–13h** was overall similar to the benzyloxy direct comparators **12o–12p**; however, phenoxy-methyl-based PAMs **13g–13h** have a 20–30% elevated Glu max response. Despite modification of the linker, PAM activity was retained, with no evidence of allosteric agonism.

In parallel, we evaluated isomeric dihydronaphthyridinones **14–15** (Table 3), which retain the linkage site for the distal phenyl *para* to the lactam amide; however, the pyridine nitrogen is adjacent to the lactam amide in a position reminiscent of a hydrogen bond accepting (HBA) pharmacophore proposed in a related ether series by Varnes and co-workers.⁴⁸ Within both series **14** (Y = N) and series **15** (X = N) NH lactams (**14a**, **15a**), *N*-methyl analogues (**14b**, **15b**), and chiral (*R*)-3,3-dimethylbutan-2-yl substitute analogues, inspired by monocyclic ether **7**, all proved to be inactive. The lack of activity in the calcium assay for parent lactams **14a** and **15a** versus the benzyloxy comparator **12a**, in addition to western 3-fluoro congeners **13b** (inactive) versus **12c** (EC₅₀ = 225 nM), suggests that for series 12–15 wherein the distal

Table 1. SAR of 2-Alkoxy-dihydronaphthyrinones 12

Series 12

| Cmpd | R ¹ | R ² | mGlu ₅ pEC ₅₀ (±SEM) ^a | mGlu ₅ EC ₅₀ (nM) | %Glu Max (±SEM) ^b |
|------|----------------|-----------------|--|--|---------------------------------|
| 12a | | H | 5.98±0.04 | 1031 | 54±4.5 |
| 12b | | H | 5.93±0.08 | 1171 | 68±5.3 |
| 12c | | H | 6.65±0.12 | 225 | 50±3.2 |
| 12d | | H | Inactive | | |
| 12e | | H | 7.21±0.18 | 62 | 43±5.6 |
| 12f | | H | Inactive | | |
| 12g | | H | Inactive | | |
| 12h | | H | Inactive | | |
| 12i | | CH ₃ | Inactive | | |
| 12j | | <i>i</i> -Bu | Inactive | | |
| 12k | | | Inactive | | |
| 12l | | | 6.35±0.09 | 444 | 36±3.4 |
| 12m | | | 5.61±0.15 | 2473 | 39±5.1 |
| 12n | | | 5.50±0.23 | 3173 | 36±5.6 |
| 12o | | | 6.93±0.07 | 118 | 38±4.0 |
| 12p | | | 6.67±0.07 | 212 | 50±4.8 |
| 12q | | H | Inactive | | |
| 12r | | | Inactive | | |
| 12s | | | 5.56±0.09 | 2765 | 23±1.4 |
| 12t | | | Inactive | | |

^aCalcium mobilization assay using HEK293 cells stably expressing rat mGlu₅ receptors; values are the average of three or more independent determinations; Inactive, less than 10% change in calcium fluorescence compared to the EC₂₀ glutamate response. ^bExpressed as amplitude of response using 30 μ M test compound (percentage of maximal response versus 100 μ M glutamate).

phenyl is maintained *para* to the lactam amide, the heteroatom arrangement between the linker oxygen and the pyridine nitrogen within series 12 is more preferred. However, *N*-aryl analogues have a unique SAR, suggesting that in this context the central tetrahydronaphthyrinone scaffold is more critical for mGlu₅ potentiation than the nature of the linker, as 12 and 13 are equally tolerated in the context of an *N*-aryl substituent. *N*-

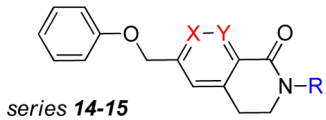
Table 2. SAR of 2-Alkoxy-methyl-dihydronaphthyrinones 13

series 13

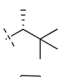
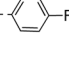
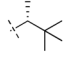
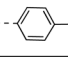
| Cmpd | R ¹ | R ² | mGlu ₅ pEC ₅₀ (±SEM) ^a | mGlu ₅ EC ₅₀ (nM) | %Glu Max (±SEM) ^b |
|------|----------------|-----------------|--|--|---------------------------------|
| 13a | | H | >5.0 | >10,000 | 43±3.4 |
| 13b | | H | >5.0 | >10,000 | 34±4.2 |
| 13c | | CH ₃ | Inactive | | |
| 13d | | <i>i</i> -Bu | 5.94±0.05 | 1146 | 38±2.9 |
| 13e | | | >5.0 | >10,000 | 33±2.0 |
| 13f | | | 6.70±0.07 | 198 | 68±1.0 |
| 13g | | | 7.01±0.07 | 97 | 72±3.9 |
| 13h | | | 6.23±0.06 | 595 | 59±2.4 |
| 13i | | | >5.0 | >10,000 | 38±0.8 |

^aCalcium mobilization assay using HEK293 cells stably expressing rat mGlu₅ receptors; values are the average of three or more independent determinations; Inactive, less than 10% change in calcium fluorescence compared to the EC₂₀ glutamate response. ^bExpressed as amplitude of response using 30 μ M test compound (percentage of maximal response versus 100 μ M glutamate).

4-Fluorophenyl PAMs 14d and 15d, which differ in the location of the central pyridine nitrogen, have comparable potency with dissimilar efficacy, with pyridine isomer 14d being one of the most efficacious PAMs reported across the tetrahydronaphthyrinone subseries described. The related congener 13f was ~2.5-fold more potent (EC₅₀ = 198 nM) with 68% glutamate max, and 13g was 2-fold more potent than 13f. Relative to series 12, 12o is equipotent to 13g; however, 13g revealed a ~2-fold higher maximal glutamate response (72% vs 38%). Although a more comprehensive survey was undertaken for series 12–13 relative to 14–15, on the basis of direct comparisons, general trends were noted between the series. A summary of the potency and efficacy profiles are found within Figure 3. Neither molecular switches nor allosteric agonism proved to be issues for 12–15 and SAR was generally steep. Active compounds within 12–13 have capacity for high potency (EC₅₀ ≤ 200 nM) and moderate to high efficacy (% Glu max ≥50%), whereas actives within series 14–15, although more limited, exhibited moderate potency and variable efficacy (%Glu max 30% and 81%). Subtle changes in structure–efficacy/cooperativity relationships are best addressed via glutamate fold-shift experiments; however, glutamate max trends were consistent within series 12–15, and series 12 shows variable efficacies that encompass the full range reported for all subseries (Figure 3). In general, phenoxy linkages show improved efficacy over benzyloxy linkages for *N*-arylated analogues. The emerging pharmacophore for 12–13 suggested these dihydronaphthyrinone scaffolds interact at the allosteric

Table 3. SAR of Isomeric Phenoxy-methyl-dihydronaphthylidones 14–15


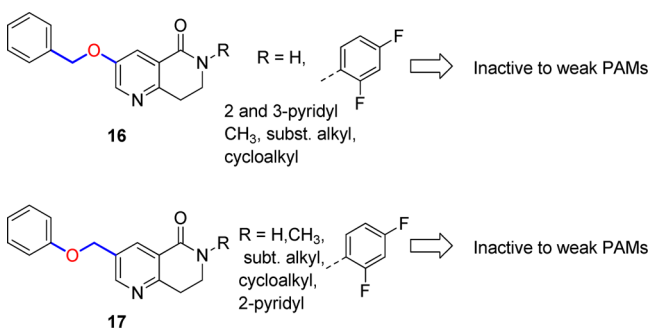
series 14–15

| Cmpd | X | Y | R | mGlu ₅ pEC ₅₀ (±SEM) ^a | mGlu ₅ EC ₅₀ (nM) | %Glu Max (±SEM) ^b |
|------|----|----|---|--|--|---------------------------------|
| 14a | CH | N | H | Inactive | | |
| 14b | CH | N | CH ₃ | Inactive | | |
| 14c | CH | N |  | Inactive | | |
| 14d | CH | N |  | 6.27±0.09 | 538 | 81±6.7 |
| 15a | N | CH | H | Inactive | | |
| 15b | N | CH | CH ₃ | Inactive | | |
| 15c | N | CH |  | Inactive | | |
| 15d | N | CH |  | 6.39±0.35 | 403 | 30±4.1 |

^aCalcium mobilization assay using HEK293 cells stably expressing rat mGlu₅ receptors; values are the average of three or more independent determinations; Inactive, less than 10% change in calcium fluorescence compared to the EC₂₀ glutamate response. ^bExpressed as amplitude of response using 30 μ M test compound (percentage of maximal response versus 100 μ M glutamate).

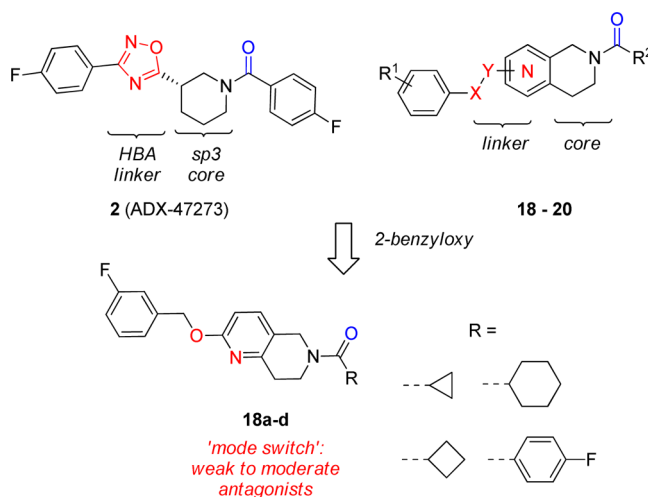
site in a manner distinct than that proposed by Varnes and co-workers⁴⁸ and likely more similar to a monocyclic series of nicotinamides previously described.²⁶ Although formally benzyloxy variants of 14 and 15 (Figure 3) remained as potential mGlu₅ PAMs, the template was not pursued. This decision was made in part on the basis of the overall efficacy and potency observed within subseries 13, thus phenoxy-based systems remained higher priority for the remaining survey.

We next pursued alternative sites for linker attachment of the pendant aryl examining 3-substituted dihydronaphthylidones based on either a benzyloxy (16) or phenoxy-based (17) system (Figure 4). Brief surveys of both *N*-alkyl and *N*-aryl and heteroaryl substituents, including several congeners related to those previously described (Table 1–3), were unsuccessful in identifying favorable starting points and led to modulators

**Figure 4.** SAR summary of 3-benzyloxy and 3-phenoxy-methyl-dihydronaphthylidones 16–17.

which were either inactive or weak PAMs (EC₅₀ > 10 μ M). Interestingly, a related more rigid, acetylene tetralone scaffold recently reported by Merz Pharmaceuticals GmbH⁵¹ displays a similar array of HBA moieties and was reported to have excellent PAM activity (EC₅₀ < 100 nM) in a recombinant CHO cell line expressing human mGlu₅.

Acyl-tetrahydronaphthylidones. Inspired in part by the Addex piperidine chemotype 2,^{15,52} we postulated that perhaps a more extended pharmacophore placing the amide carbonyl moiety exocyclic of the tetrahydronaphthylidone scaffold as found within the Addex chemotype might prove viable (Figure 5). PAM 12c served as a precursor (Scheme 1) and allowed for

**Figure 5.** Relationship between 2 and 18–20 and resulting first-generation exocyclic amides 18 utilizing 2-benzyloxy linkage.

facile access to representative benzyloxy targets 18a–d in two steps via borane reduction and subsequent amide coupling. Intriguingly, all proved to be weak to moderate antagonists of mGlu₅ (Figure 5). At this juncture, in light of the unexpected switch in the mode of pharmacology for subseries 18, as well as the general challenges of multidimensional combinations of linker, core, attachment site, and lactam versus exocyclic amide (minimum of 24 formal combinations/scaffolds), we employed a ligand-based computational tool previously reported⁴² to prioritize and potentially streamline medicinal chemistry efforts and ligand design. Using this approach, we assessed ligand-based conformational ensembles of known highly efficacious PAMs, including Addex ligand 2⁵² and other lead molecules,^{53,54} with PAM activity below 150 nM and robust Glu max values above 70%. These low energy ensembles of PAMs served as flexible “hypotheses” or reference PAMs for a mutual flexible low energy shape-based alignment of proposed dihydronaphthylidone and tetrahydronaphthylidones using the Surflex-Sim algorithm as implemented in Sybyl.^{55,56} The molecular similarity and alignment optimization algorithms used in Surflex-Sim docking utilize a functional term to minimize the volume of molecular superpositions to construct an objective function for scoring superpositions of multiple molecules. The objective function can then be used as targets for virtual screening, or in this case, for scaffold hopping prioritization. The results from these studies using 2 are summarized in Figure 6 with a depicted overlay of the lowest energy structures for 2 versus 2-phenoxy methyl model amide 19 and 3-phenoxy methyl model amide 20. A Surflex-Sim score

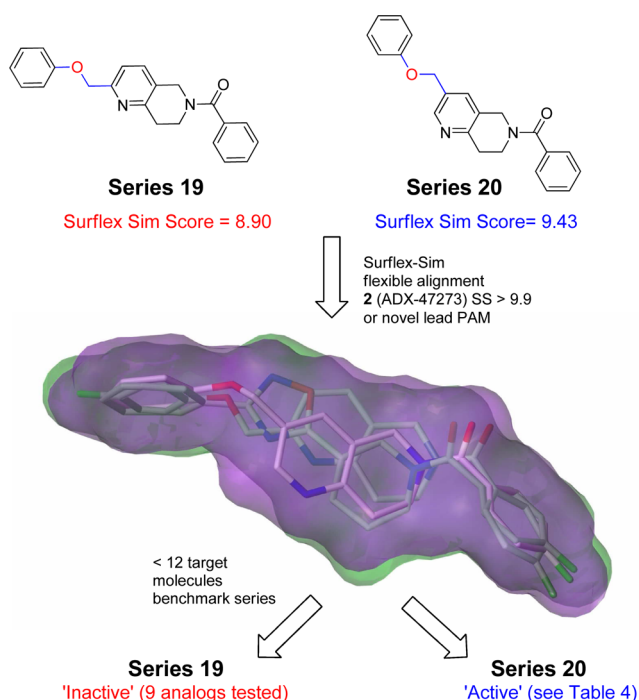


Figure 6. Example of flexible alignment of model 2 and 3-phenoxy-methyl-tetrahydronaphthyridines **19** and **20** (green surface) vs **2** (purple surface).

(SS) that approaches the reference hypothesis, arbitrarily set to 10, is indicative of a template that more closely mimics the reference conformer ensemble. Using **2** as a template, series **20**, containing a 3-phenoxy-methyl, was predicted to have greater molecular similarity (SS = 9.43) than the 2-phenoxy-methyl prototype **19** (SS = 8.90). Unlike 2-benzyloxy derivatives within series **18**, compounds within series **19** were not antagonists and proved inactive in the primary calcium assay (nine analogues were prepared and tested from a 3-fluoro 1-(2-((3-fluorophenoxy)methyl)-7,8-dihydro-1,6-naphthyridin-6(SH)-yl)ethanone scaffold, see Supporting Information); however, at this time, it is unclear if compounds within series **19** have neutral cooperativity and thus retained affinity for mGlu₅ (a silent allosteric modulator or SAM).^{44,57} With this caveat in mind, it is also recognized that the PAM EC₅₀ is better described as a composite of four parameters encompassing affinity of the modulator for the receptor, allosteric effects on binding and signaling of the orthosteric ligand and potential intrinsic agonist efficacy of the modulator. Thus, although within closely related series, the Surflex-Sim approach appears to facilitate scaffold prioritization based on PAM EC₅₀ activity at of Glu₅, the power of the Surflex-Sim methodology warrants a broader more rigorous retrospective analysis with these additional facets of modulator activity taken into consideration.

With some insight that perhaps 3-substituted tetrahydronaphthyridines **20** were preferred from ligand-based modeling, additional analogues were prioritized. Selected derivatives **20a**–**20c**, which retains a 3-phenoxy methyl linker, and 3-benzyloxy variants **20d**–**20g**, are shown in Table 4. Within benzyloxy derivatives **20d**–**20g**, compounds covered a spectrum of profiles ranging from inactive (**20d**, **20f**), to weak PAMs (**20e**), to weak partial antagonists (**20g**); the latter effect driven by subtle changes in fluorine substitution patterns, a phenomenon not uncommon among certain mGlu₅ modulator chemotypes.³³ Within the phenoxy subseries analogues **20a**–

Table 4. “Exocyclic” Tetrahydronaphthyridine Amides **20**

| series 20 | | | | | | |
|------------------|----|---------------------|---|--|--|---------------------------------|
| Cmpd | Ar | X-Y | R | mGlu ₅ pEC ₅₀ (±SEM) ^a | mGlu ₅ EC ₅₀ (nM) | %Glu Max (±SEM) ^b |
| 20a | | -OCH ₂ - | | 6.19±0.09 | 640 | 69±3.9 |
| 20b | | -OCH ₂ - | | 5.96±0.10 | 1090 | 69±5.9 |
| 20c | | -OCH ₂ - | | 5.75±0.02 | 1770 | 53±3.1 |
| 20d | | -CH ₂ O- | | Inactive | | |
| 20e | | -CH ₂ O- | | 5.79±0.09 | 1634 | 30±4.7 |
| 20f | | -CH ₂ O- | | Inactive | | |
| 20g | | -CH ₂ O- | | 5.11±0.09 ^c | 7815 ^c | 53±1.1 ^c |

^aCalcium mobilization assay using HEK293 cells stably expressing rat mGlu₅ receptors; values are the average of three or more independent determinations; Inactive, less than 10% change in calcium fluorescence compared to the EC₂₀ glutamate response. ^bExpressed as amplitude of response using 30 μM test compound (percentage of maximal response versus 100 μM glutamate). ^cWeak antagonist, data represents pLC₅₀/IC₅₀ from EC₈₀ window and %Glu represents E_{min} not E_{max}.

20c, success was found with 4-fluorobenzamide derivatives; in particular, the western phenyl and 3-fluoro phenyl derivatives **20a** and **20b** have statistically comparable potency and efficacy, with EC₅₀s of 640 and 1090 nM, respectively, and a Glu max of 69%. In contrast, the 4-fluoro congener **20c** was 2–3-fold less active. Three significant findings are evident among these lactam and exocyclic amide templates examined: (1) parent dihydronaphthyridinone **12c** remains a confounding singleton relative to regioisomeric and positional congeners **13b**, **14a**, **15a**, **16**, and **17**, (2) relative to earlier acetylenic dihydronaphthyridinones **11**,³² no molecular switches were noted within dihydronaphthyridinone systems, however, steep SAR was evident, and (3) in contrast to dihydronaphthyridinones, exocyclic acyl-tetrahydronaphthyridines were highly sensitive to the linker attachment site, as 2-substituted based ethers **18** and **19**, proved to be either weak antagonists or functionally inactive in the calcium assay. In addition, within the exocyclic acyl-tetrahydronaphthyridines, phenoxy-methyl-based ethers were better tolerated and less susceptible to changes in the mode of pharmacology (e.g., **20a** versus **20g**); however, overall potency was generally diminished relative to series **12**–**13**.

In light of the overall mGlu₅ PAM potency (EC₅₀ < 250 nM) and efficacy (Glu max >50%) observed for compounds **12c**, **12p**, **13f**, and **13g**, these PAMs were selected for further characterization (Table 5). In addition, the moderately potent PAM **14d** (EC₅₀ = 538 nM) was considered for further evaluation based upon its enhanced efficacy (Glu max = 81%).

Among the PAMs further examined, **12p**, **13f**, **13g**, and **14d** have similar cLogP and molecular weight (MW) by virtue of their common lactam *N*-aryl substituent, while the simple NH lactam **12c** stands out as a low MW modulator (MW = 272) with excellent calculated ligand efficiency metrics (LipE and LELP, see Table 5).^{58,59} PAM **12c** maintains the highest

Table 5. Rat mGlu₅ Potency Values and Data for Selected Key Compounds

| compd | rmGlu ₅ EC ₅₀ ^a (nM) | cLogP ^b | LipE ^c | LELP ^c | CL _{int} (h, r) ^d | CL _{HEP} (h, r) ^d | PPB f _u (h, r) ^e |
|-------|---|--------------------|-------------------|-------------------|---------------------------------------|---------------------------------------|--|
| 12c | 225 | 2.62 | 4.03 | 5.76 | 25/175 | 11/50 | 0.047/0.034 |
| 12p | 212 | 3.96 | 2.71 | 11.71 | 18/138 | 9.6/47 | 0.010/0.025 |
| 13f | 198 | 3.72 | 2.98 | 10.55 | 18/108 | 9.6/43 | 0.021/0/036 |
| 13g | 97 | 3.88 | 3.13 | 10.92 | 8.8/121 | 6.2/44 | 0.014/0.029 |
| 14d | 538 | 3.60 | 2.67 | 10.92 | 19/33 | 10/22 | 0.096/0.110 |

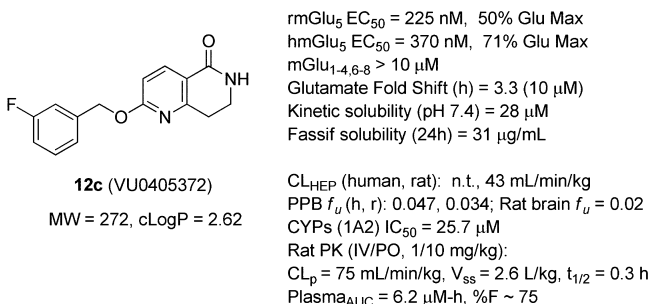
^aFor the mGlu₅ pEC₅₀ assay see Tables 1–4 and Experimental Section. ^bcLogP was calculated using Adriana's XLogP code. ^cLipE = pEC₅₀–cLogP; LELP = ligand efficiency/cLogP.^{58,59} ^dCL_{int}, intrinsic clearance; CL_{HEP}, predicted hepatic clearance, human and rat (h, r), mL/min/kg. ^ePPB f_u, plasma protein binding fraction unbound.

calculated LipE and lowest LELP among the set, suggesting a highly favorable enthalpy driven effect on cooperativity. Despite the less favorable physicochemical and LE properties for **12p**, **13f**, **13g**, and **14d** relative to **12c**, intrinsic clearance in human and rat microsomes suggested moderate predicted hepatic clearance and 1–10% fraction unbound. Subsequent selectivity profiling against mGlu_{1–4,6–8} using **12c**, **13g**, and **14d** revealed that *N*-aryl congeners **13g** and **14d** were also active as mGlu₃ negative allosteric modulators (NAMs) with negative cooperativity fold-shift values between 0.2 and 0.3, while **12c** was fully selective for mGlu₅ (mGlu_{1–4,6–8} EC₅₀ > 10 μ M, see Supporting Information).

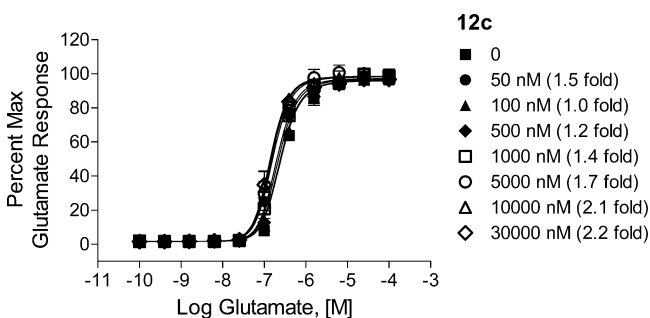
Additional Pharmacological Characterization of 12c. In light of the unexpected lack of selectivity for **13g** and **14d** which maintain a similar *N*-aryl endocyclic amide pharmacophore found within **12p** and **13f**, we elected to continue to profile **12c** in more depth based on its overall potency, selectivity, and excellent physicochemical and ligand efficiency parameters (see Figure 7 for overall profile). Positive allosteric

mGlu₅ receptor revealed a small leftward shift in the glutamate concentration response curve (CRC) with increasing concentration of **12c** (55 nM to 30 μ M), with no significant effect on the maximal response. A 2.2-fold leftward shift in the glutamate EC₅₀ was observed in the presence of 30 μ M **12c**, and a predicted allosteric modulator affinity of 2.17 μ M and an efficacy cooperativity factor (log β) between glutamate and indicated allosteric modulator of 0.23 (cooperativity \sim 1.71) was defined as calculated using the operational model of allosterism.⁶⁰ These results support a positive allosteric interaction between glutamate and **12c** and were confirmed in a cell line expressing the human mGlu₅ receptor,⁴⁶ where 10 μ M **12c** produced a 3.3-fold leftward shift in the glutamate CRC and a PAM CRC potency of 370 nM (71% Glu max). In comparison to recently reported PAMs from our lab that have been profiled in glutamate progressive fold-shift studies up to 30 μ M, including acetylenic picolinamides (e.g., ML254, maximum rat mGlu₅ fold-shift 3.0)³⁰ and dihydrothiazolopyridone **10** (maximum rat mGlu₅ fold-shift 5.4),³¹ **12c** represents one of the weakest mGlu₅ allosteric modulators reported in terms of measurable positive cooperativity.

Extended DMPK Characterization and Ancillary Pharmacology of 12c. Rat brain homogenate binding to assess fraction unbound in brain revealed a reasonable brain f_u of 2.0% for **12c**. Inhibition of the major human cytochrome P450 (CYP) enzymes (2C9, 2D6, 3A4, 1A2) was measured in a cocktail assay using human liver microsomes and known substrates. PAM **12c** was found to display weak CYP inhibitory activity at 1A2 (IC₅₀ = 25.7 μ M), while no activity was observed against the other CYPs tested (IC₅₀ > 30 μ M). In kinetic aqueous solubility assays, **12c** displayed moderate to good solubility (pH 2, 4, 7.4 buffer: 38, 29, and 28 μ M) and moderate solubility in fasted simulated intestinal fluid (Fassif, pH = 7.2) of 31 μ g/mL (114 μ M). In a nontoxic vehicle screen using 20% HP β -cyclodextrin, **12c** was a solution at 1 mg/mL and a microsuspension at 3–5 mg/mL (pH 4.0). Rat pharmacokinetic studies (1 mg/kg IV, 10 mg/kg PO) revealed a high plasma clearance (CL_p) of 75 mL/min/kg and a short half-life (T_{1/2}) of 0.3 h. After oral administration (10 mg/kg, 0.5% methyl cellulose, 1 mg/mL, noncrossover) to male Sprague–Dawley rats, **12c** reached an average maximal concentration (C_{max}) of 3.36 μ M with a corresponding time to reach C_{max} (T_{max}) of 0.5 h and an AUC_{0–24h} of 6.2 μ M-h, thus affording an estimated %F of 75. We performed a single dose in vivo screen to study the ability of **12c** to reverse amphetamine-induced hyperlocomotion in rats (PO, 56.6 mg/kg 20% HP β -cyclodextrin). Robust reversal of the hyperlocomotion response was noted at this dose (>30%, data not shown) and high brain exposure was observed at 1.5 h (C_{brain} = 16.6 μ M, 332 nM unbound), producing an average brain-to-plasma (B:P) ratio of 1.67 and unbound brain level above the rat in vitro EC₅₀.

Figure 7. Profile summary of **12c**.

modulator activity was investigated by fold-shift experiments to determine the degree of cooperativity with glutamate. As shown in Figure 8, progressive fold-shift experiments utilizing the rat

Figure 8. Glutamate CRC in the presence of increasing concentrations of **12c**.

Furthermore, in vivo B:P and in vitro $f_{u,plasma}/f_{u,brain}$ (1.7) measures were identical, with a calculated $K_{p,uu}$ of 1.1, suggesting passive CNS penetration for **12c** in rat.⁶¹ Thus, **12c** continued to demonstrate promising properties to warrant further evaluation in vivo. With respect to ancillary pharmacology, in a broad panel selectivity screen against 68 GPCRs, ion channels and transporters using 10 μ M **12c**, no significant off-target activity was noted (Eurofins Inc.).

In Vivo Pharmacological Characterization. Encouraged by its overall profile as a low fold-shift PAM, **12c** was evaluated across a range of doses for its ability to reverse amphetamine-induced hyperlocomotion (AHL), an established model of antipsychotic activity (Figure 8).^{17,36} As seen in Figure 9, **12c**

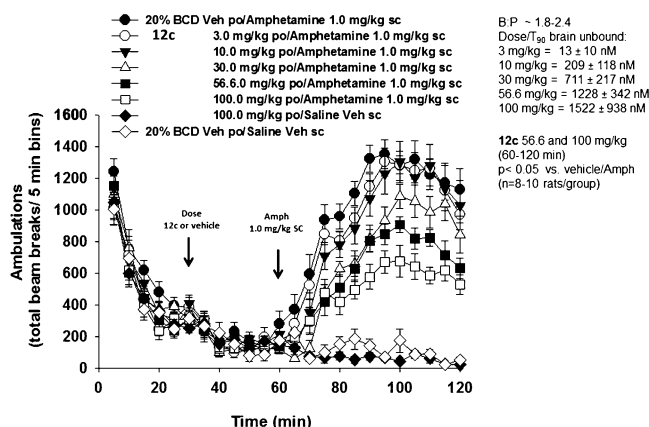


Figure 9. Dose-dependent effect and calculated terminal unbound brain of **12c** on the reversal of amphetamine-induced hyperlocomotion in rats.

dosed orally showed robust dose-dependent effects in reversal of hyperlocomotion, with a maximal effect (55%) observed at the highest dose tested of 100 mg/kg and an average terminal unbound brain concentration of 1.5 μ M. The lowest active dose of 30 mg/kg afforded an estimated average terminal unbound brain concentration of ~712 nM, which represents a 3-fold multiple of the rat in vitro potency and according to the progressive fold-shift studies (Figure 8), represents a left-ward shift in the glutamate CRC in the ~1.2–1.4 fold range. Despite the overall low positive cooperativity, **12c** retains efficacy in AHL at unbound brain exposures that are a multiple of the in vitro EC_{50} and thus illustrates that high cooperativity with glutamate is not fully required for an mGlu₅ PAM to maintain activity in the AHL model. This observation appears to be in contrast to data reported recently for low fold-shift PAMs **8–9** reported by Lilly, wherein little effect was noted in a similar amphetamine-induced hyperlocomotor activity assay using male Lister hooded rats.²³ Rotarod studies were performed using **12c** at a doses of 30, 56.6, and 100 mg/kg PO (20% HP- β -CD in water) to assess balance and motor coordination (see Supporting Information). PAM **12c** showed no statistically significant effect on general motor output (120 s cutoff). In a modified Irwin neurological test battery in rats, **12c**, when dosed at 100 mg/kg PO (20% HP- β -CD in water), had no performance deficits on any autonomic or somatomotor nervous system functions out to 4 h. Collectively, these results highlight that PAM **12c** is free from overt neurological side effects and motor behavior deficits at doses that produce maximal efficacy in reversal of amphetamine-induced hyperlocomotion (100 mg/kg PO).

CONCLUSIONS

Diverse mGlu₅ modulator pharmacological profiles were attained within a series of tetrahydronaphthyridine and dihydronaphthyridinone scaffolds through modifications of heteroatoms within the linker, core structure, and location of the pendant linkage moiety. Up to 10 diverse subseries were examined, and five of these series, **12–15** and **20**, were described in detail, leading to preferred endocyclic series **12** and **13** which, although free from allosteric agonism and molecular switches, tended to have steep SAR. N-Aryl dihydronaphthyridinone congeners were nonselective and displayed negative cooperativity at mGlu₃ and thus were not further progressed. Parent benzyloxy lactam **12c** emerged as a suitable tool compound with good potency, excellent selectivity, and pharmacokinetic properties suitable for acute studies. Despite behaving in vitro as an ultralow cooperativity PAM in recombinant systems, **12c** showed robust, dose-dependent effects in the reversal of amphetamine-induced hyperlocomotion, with a lowest active dose of 30 mg/kg PO, that produced an estimated brain unbound level 3-fold above its in vitro potency. Maximal efficacy of **12c** was observed at a dose of 100 mg/kg with no significant motor impairment or overt neurological side effects. **12c** provides another tool compound to complement the available mGlu₅ PAMs with well characterized cooperativity profiles^{30,31} to better enable comparative studies with other chemotypes in native systems and in preclinical animal models.

EXPERIMENTAL SECTION

General. All reagents purchased from commercial suppliers were used without purification. Unless noted, all solvents used were anhydrous and all reactions were carried out under argon atmosphere. Microwave assisted reactions were performed in a single-mode reactor: Emrys Optimizer microwave reactor (Biotage). Analytical thin layer chromatography was performed on Analtech silica gel GF 250 μ m plates and on silica gel 60 F254 plates (Merck) under standard techniques. Unless otherwise specified, preparative reverse-phase high performance liquid chromatography (RP-HPLC) purification was performed on a Gilson Inc. preparative UV-based system using a Phenomenex Luna C18 column (50 mm \times 30 mm I.D., 5 μ m), with an acetonitrile (unmodified)–0.1% trifluoroacetic acid in water gradient. Normal-phase silica gel preparative purification was performed using an automated Combi-flash Rf from ISCO using either ISCO or Merck ready-to-connect cartridges. Analytical LC/MS was performed using the following instruments: (A) Agilent 1200 series with UV detection at 215 and 254 nm and ELSD detection (Polymer Laboratories PL-ELS 2100), utilizing an Accucore C18 2.6 μ , 2.1 mm \times 30 mm column, a 1.1 min gradient, 7% [CH_3CN /0.1% TFA]–95% [CH_3CN /0.1% TFA] and a G6130 single quadrupole mass spectrometer or (B) ultra performance liquid chromatography (UPLC) measurement performed using an Acquity UPLC (Waters) system comprising a sampler organizer, a binary pump with degasser, a four column's oven, a diode array detector (DAD), and a BEH-C18 column (1.7 μ m, 2.1 mm \times 50 mm) from Waters, with a flow rate of 1.0 mL/min at 50 $^{\circ}C$ without split to the MS detector. The gradient conditions consisted of 95% A (0.5 g/L ammonium acetate solution + 5% acetonitrile), 5% B (acetonitrile), to 40% A, 60% B in 3.8 min, to 5% A, 95% B in 4.6 min, kept until 5.0 min without split to the MS detector. The MS detector was configured with an ESCI dual ionization source (electrospray combined with atmospheric pressure chemical ionization). Nitrogen was used as the nebulizer gas. The source temperature was maintained at 140 $^{\circ}C$. Low-resolution mass spectra (single quadrupole, SQD detector) were acquired by scanning from 100 to 1000 in 0.1 s using an interchannel delay of 0.08 s. The capillary needle voltage was 3 kV. The cone voltage was 25 V for positive ionization mode and 30 V for negative ionization mode. Data

acquisition was performed with MassLynx-Openlynx software. GC/MS measurement was performed using a 6890 series gas chromatograph (Agilent Technologies) system comprising a 7683 series injector and autosampler, coupled to a 5973N MSD mass selective detector (single quadrupole, Agilent Technologies). The MS detector was configured with an electronic impact ionization source/chemical ionization source (EI/CI). EI low-resolution mass spectra were acquired by scanning from 50 to 550 at a rate of 14.29 scans/s. The source temperature was maintained at 230 °C. Helium was used as the nebulizer gas. Data acquisition was performed with Chemstation-Open Action software. GC/MS was carried out on a J&W HP-5MS column (20 m × 0.18 mm, 0.18 μm) from Agilent Technologies, with a flow rate of 0.7 mL/min. The temperature gradient applied was: initial temperature 50 °C, hold for 2.0 min, then a 50 °C/min ramp applied for 5.0 min until 300 °C and hold for 3.0 min in a 10 min run. Front inlet temperature was 250 °C. Split injection mode was used, 0.2 μL injection volume, with a 50/1 ratio into the GC/MS system. HRMS were obtained using a Micromass (Waters) Q-ToF API-US calibrated and verified with sodium iodide. The samples were diluted with a 50:50 0.1% formic acid (in Milli-Q):acetonitrile solution, directly infused using leucine-enkephalin (M + H = 556.2771) as a lockmass. Scan range was from 100 to 1000 Da, using a scan time of one second. The [M + H] or [M + Na] ion was observed. Purity of all final compounds was determined to be >98% by HPLC. Solvents for extraction, washing, and chromatography were HPLC grade. NMR spectra were recorded on either a Bruker DPX-400 or a Bruker AV-500 MHz spectrometer with standard pulse sequences. ¹H chemical shifts are reported as δ values in CDCl₃ or DMSO-*d*₆. Data are reported as follows: chemical shift, integration, multiplicity (s = singlet, bs = broad singlet, d = doublet, t = triplet, q = quartet, p = pentet, hex = hexet, sep = septet, dd = doublet of doublets, dt = doublet of triplets, dq = doublet of quartets, m = multiplet), coupling constant *J* reported in Hz. ¹³C chemical shifts are reported in δ values in CDCl₃ as follows: chemical shift, C–F coupling constants (*J*_{C–F}) reported in Hz. For a number of compounds, melting points (mp) were determined in open capillary tubes on a FP62 or on a FP81HTFP90 apparatus (Mettler). Melting points were measured with a temperature gradient of 10 °C/min (maximum temperature 300 °C), and the melting point was read from a digital display. Melting point values are peak values and were obtained with experimental uncertainties that are commonly associated with this analytical method. Optical rotation values were obtained on a JASCO P-2000 polarimeter.

Chemistry. Synthesis of presented compounds was performed according to Schemes 1–6. Experimental procedures, analytical data, HRMS, and NMR spectra can be found within Supporting Information. Synthesis and analytical data for representative members within series 12–19 are provided below.

2-(Benzyloxy)-7,8-dihydro-1,6-naphthyridin-5(6H)-one (12a). Benzyl alcohol (85 μL, 0.82 mmol) was dissolved into DMF (1.6 mL) and treated with KOt-Bu (184 mg, 1.64 mmol) and stirred for 30 min. The mixture was treated with 2-chloro-7,8-dihydro-1,6-naphthyridin-5(6H)-one (**20**, 100 mg, 0.55 mmol, see Supporting Information) and heated to 100 °C for 4 h. The mixture was cooled to rt, acidified with 6 N HCl, and extracted with EtOAc (3×). The combined organic layers were washed with brine, dried over Na₂SO₄, and evaporated to dryness. The crude product mixture was purified by RP-HPLC (eluting with 40–90% MeCN/H₂O with 0.1% TFA modifier) to afford the title compound (73 mg, 53%). ¹H NMR (400 MHz, CDCl₃) δ 8.20 (1H, d, *J* = 8.6 Hz), 7.46 (2H, m), 7.36 (3H, m), 6.75 (1H, d, *J* = 8.6 Hz), 5.85 (1H, bs), 5.43 (2H, s), 3.62 (2H, t, *J* = 6.8 Hz), 3.09 (2H, t, *J* = 6.8 Hz). ¹³C NMR (100 MHz, CDCl₃) δ 166.4, 165.2, 158.0, 138.3, 136.7, 128.4, 128.0, 127.9, 118.3, 109.8, 68.1, 39.2, 30.7. HRMS (ES+, M + H) calcd for C₁₅H₁₃N₂O₂, 255.1134, found, 255.1130.

2-((3-Fluorobenzyl)oxy)-7,8-dihydro-1,6-naphthyridin-5(6H)-one (12c). 3-Fluorobenzyl alcohol (1.66 g, 13.14 mmol) was dissolved into DMF (25 mL) and treated with KOt-Bu (3.2 g, 26.29 mmol) and stirred for 30 min. The mixture was treated with 2-chloro-7,8-dihydro-1,6-naphthyridin-5(6H)-one (**20**, 1.49 g, 8.82 mmol, see Supporting Information) and heated to 100 °C overnight. The mixture was

adsorbed onto silica and purified (0 to 80% EtOAc/hexanes) to give a semipure solid. This material was further purified on RP-HPLC (eluting with 40–90% MeCN/H₂O with 0.1% TFA modifier) to give 840 mg of the title compound (35%). ¹H NMR (400 MHz, CDCl₃) δ 8.44 (1H, d, *J* = 7.6 Hz), 7.38 (1H, dd, *J* = 14.6, 7.6 Hz), 7.24 (1H, d, *J* = 7.5 Hz), 7.22 (1H, d, *J* = 9.6 Hz), 7.04 (1H, t, *J* = 8 Hz), 6.79 (1H, d, *J* = 8.4 Hz), 5.79 (1H, br s), 5.45 (2H, s), 3.64 (2H, t, *J* = 6.4 Hz), 3.10 (2H, t, *J* = 6.4 Hz). LCMS *t*_R = 0.736 min, > 98% at 215 and 254 nm, *m/z* = 273.1 [M + H]. HRMS (ES+, M + H) calcd for C₁₅H₁₄FN₂O₂, 273.0961; found, 273.0963.

2-Butoxy-7,8-dihydro-1,6-naphthyridin-5(6H)-one (12q). Starting from 2-chloro-7,8-dihydro-1,6-naphthyridin-5(6H)-one (100 mg, 0.55 mmol) and following the general procedure outlined in **12a** and **12c**, RP-HPLC afforded the title compound as a powder (72 mg, 60%). ¹H NMR (400 MHz, CDCl₃) δ 8.17 (1H, d, *J* = 8.6 Hz), 6.67 (1H, d, *J* = 8.6 Hz), 5.84 (1H, bs), 4.33 (2H, t, *J* = 6.6 Hz), 3.61 (2H, t, *J* = 6.8 Hz), 3.06 (2H, t, *J* = 6.8 Hz), 1.77 (2H, p, *J* = 7.9 Hz), 1.48 (2H, hex, *J* = 7.5 Hz), 0.98 (3H, t, *J* = 7.4 Hz). ¹³C NMR (100 MHz, CDCl₃) δ 166.6, 165.7, 158.1, 138.1, 117.9, 109.4, 66.3, 39.2, 30.9, 30.8, 19.1, 13.7. HRMS (ES+, M + H) calcd for C₁₂H₁₇N₂O₂, 221.1290; found, 221.1290.

2-Butoxy-6-(2,4-difluorophenyl)-7,8-dihydro-1,6-naphthyridin-5(6H)-one (12r). 2-Butoxy-7,8-dihydro-1,6-naphthyridin-5(6H)-one (**12q**, 50 mg, 0.23 mmol), 1-bromo-2,4-difluorobenzene (52 μL, 0.46 mmol), CuI (9.1 mg, 0.047 mmol), *N,N*′-dimethylethane-1,2-diamine (14 μL, 0.129 mmol), and potassium carbonate (64 mg, 0.46 mmol) were combined in a 2.0 mL microwave vial and placed under an argon atmosphere. Degassed toluene was added and the mixture heated at 110 °C for 6 h. The mixture was cooled to rt, filtered over Celite, and the filtrate concentrated to dryness. RP-HPLC purification afforded the title compound as a powder (45 mg, 59%). ¹H NMR (400 MHz, CDCl₃) δ 8.22 (1H, d, *J* = 8.6 Hz), 7.32 (1H, m), 6.92 (2H, m), 6.68 (1H, d, *J* = 8.6 Hz), 4.35 (2H, t, *J* = 6.6 Hz), 3.91 (2H, t, *J* = 6.7 Hz), 3.19 (2H, t, *J* = 6.6 Hz), 1.77 (2H, p, *J* = 7.9 Hz), 1.48 (2H, hex, *J* = 7.6 Hz), 0.98 (3H, t, *J* = 7.4 Hz). ¹³C NMR (100 MHz, CDCl₃) δ 165.9, 163.9, 161.4 (dd, *J*_{C–F} = 247.6, 11.3 Hz), 157.8 (dd, *J*_{C–F} = 250.8, 12.3 Hz), 157.66, 139.00, 129.61 (dd, *J*_{C–F} = 9.8, 2.6 Hz), 126.42, (dd, *J*_{C–F} = 12.8, 3.9 Hz), 118.0, 111.55 (dd, *J*_{C–F} = 22.2, 3.6 Hz), 109.7, 104.9 (dd, *J*_{C–F} = 26.0, 24.0 Hz), 66.4, 48.5, 31.2, 31.0, 19.2, 13.8. HRMS (ES+, M + H) calcd for C₁₈H₁₉F₂N₂O₂, 333.1415; found, 333.1413.

6-Benzyl-2-(benzyloxy)-7,8-dihydro-1,6-naphthyridin-5(6H)-one (12s). 2-(Benzyloxy)-7,8-dihydro-1,6-naphthyridin-5(6H)-one (**12a**, 30 mg, 0.117 mmol) and benzyl bromide (19 μL, 0.158 mmol) were dissolved into DMF (0.5 mL) and KOt-Bu added (16 mg, 0.143 mmol). The mixture was stirred for 3 h at 60 °C and then cooled to rt. Water (1.0 mL) was added to the mixture and extracted with EtOAc (3×). The combined organic layers were evaporated to dryness and the crude product mixture purified by RP-HPLC to afford 16 mg of the desired product (40%). ¹H NMR (400 MHz, CDCl₃) δ 8.28 (1H, d, *J* = 8.6 Hz), 7.45 (2H, m), 7.33 (8H, m), 6.76 (1H, d, *J* = 8.6 Hz), 5.41 (2H, s), 4.77 (2H, s), 3.53 (2H, t, *J* = 6.9 Hz), 3.02 (2H, t, *J* = 6.9 Hz). ¹³C NMR (100 MHz, CDCl₃) δ 165.1, 164.1, 156.9, 139.0, 137.3, 136.8, 128.7, 128.5, 128.1, 128.0, 127.9, 127.5, 118.7, 109.9, 68.1, 50.2, 44.5, 30.7. HRMS (ES+, M + H) calcd for C₂₂H₂₁N₂O₂, 345.1603; found, 345.1600.

2-(Benzyloxy)-6-(pyridin-2-ylmethyl)-7,8-dihydro-1,6-naphthyridin-5(6H)-one (12t). 2-(Benzyloxy)-7,8-dihydro-1,6-naphthyridin-5(6H)-one (**12a**, 30 mg, 0.117 mmol) and 2-bromomethylpyridine-hydrogenbromide (40 mg, 0.158 mmol) were dissolved into DMF (0.5 mL) and KOt-Bu added (36 mg, 1.35 mmol). The mixture was stirred for 3 h at 60 °C and then cooled to rt. Water (1.0 mL) was added to the mixture and extracted with EtOAc (3×). The combined organic layers were evaporated to dryness and the crude product mixture purified by RP-HPLC to afford 16.2 mg of **12t** (40%). ¹H NMR (400 MHz, CDCl₃) δ 0.855 (1H, d, *J* = 4.6 Hz), 8.25 (1H, d, *J* = 8.6 Hz), 7.66 (1H, dt, *J* = 7.6, 1.7 Hz), 7.45 (2H, m), 7.35 (4H, m), 7.2 (1H, m), 6.74 (1H, d, *J* = 8.6 Hz), 5.41 (2H, s), 4.88 (2H, s), 3.70 (2H, t, *J* = 6.9 Hz), 3.07 (2H, t, *J* = 6.9 Hz). ¹³C NMR (100 MHz, CDCl₃) δ 165.1, 164.2, 157.3, 157.2, 149.2, 140.0, 136.9, 136.8, 128.5, 128.1,

128.0, 122.4, 122.3, 118.6, 109.8, 68.1, 52.4, 45.6, 30.7. HRMS (ES⁺, M + H) calcd for C₂₁H₂₀N₂O₂, 346.1556; found, 346.1553.

2-(Phenoxy)methyl-7,8-dihydro-1,6-naphthyridin-5(6H)-one (13a). [2-(Phenoxy)methyl]-6-(4-methoxybenzyl)-7,8-dihydro-1,6-naphthyridin-5(6H)-one (14 mg, 0.037 mmol) was dissolved in CH₃CN (0.25 mL) and water (0.1 mL) added. Cerium ammonium nitrate (24.3 mg, 0.04 mmol) was added, and after 15 min, the reaction was partitioned between EtOAc (5 mL) and brine (1 mL). The mixture was extracted with EtOAc (2×), and the organic layers combined, concentrated, and purified by RP-HPLC to give title compound (2.6 mg, 28%). ¹H NMR (400 MHz, CDCl₃) δ 8.32 (1H, d, J = 8.0 Hz), 7.49 (1H, d, J = 8.0 Hz), 7.25 (2H, m), 6.76 (1H, m), 6.69 (2H, m), 6.49 (1H, bs), 5.10 (2H, s), 3.65 (2H, d, J = 6.9, 2.5 Hz), 3.20 (2H, t, J = 6.7 Hz). LCMS t_R = 0.732 min, > 98% at 215 and 254 nm, m/z = 255.1 [M + H]. HRMS (ES⁺, M + H) calcd for C₁₅H₁₄N₂O₂, 255.1055; found, 255.1057.

2-((3-Fluorophenoxy)methyl)-7,8-dihydro-1,6-naphthyridin-5(6H)-one (13b). [2-((3-Fluorophenoxy)methyl)-6-(4-methoxybenzyl)-7,8-dihydro-1,6-naphthyridin-5(6H)-one (23b, 300 mg, 0.77 mmol) was dissolved in CH₃CN (5 mL) and water (2 mL) added. Cerium ammonium nitrate (419 mg, 0.77 mmol) was added, and after 15 min, the reaction was partitioned between EtOAc (10 mL) and brine (10 mL). The organic layers were concentrated and purified by RP-HPLC to give title compound as a solid (74 mg, 76%). ¹H NMR (400 MHz, CDCl₃) δ 8.36 (1H, d, J = 8.0 Hz), 7.53 (1H, d, J = 8.0 Hz), 7.25 (1H, m), 6.76 (1H, m), 6.69 (2H, m), 6.49 (1H, bs), 5.20 (2H, s), 3.68 (2H, dt, J = 6.7, 2.5 Hz), 3.21 (2H, t, J = 6.7 Hz). ¹³C NMR (100 MHz, CDCl₃) δ 165.3, 163.6 (d, J_{C-F} = 244.2 Hz), 159.9, 159.4 (d, J_{C-F} = 10.9 Hz), 158.3, 136.8, 130.4 (d, J_{C-F} = 9.8 Hz), 123.9, 119.9, 110.5 (d, J_{C-F} = 2.9 Hz), 108.3 (d, J_{C-F} = 21.1 Hz), 102.7 (d, J_{C-F} = 24.9 Hz), 70.5, 39.4, 30.9. HRMS (ES⁺, M + H) calcd for C₁₅H₁₄FN₂O₂, 273.1039; found, 273.1037.

2-((3-Fluorophenoxy)methyl)-6-methyl-7,8-dihydro-1,6-naphthyridin-5(6H)-one (13c). 2-((3-Fluorophenoxy)methyl)-7,8-dihydro-1,6-naphthyridin-5(6H)-one (13b) (10.0 mg, 0.04 mmol) was dissolved in DMF (0.5 mL). NaH (2.0 mg, 0.08 mmol) was added into the solution and stirred at rt. After 30 min, MeI (5.0 μL) was added into the mixture and allowed to stir for 1 h. The mixture was then quenched with H₂O (2.0 mL) and extracted with EtOAc (3×). The organic layers were combined and concentrated to afford product as a white solid (9.2 mg, 87%). LCMS t_R = 0.81 min, > 98% at 215 and 254 nm, m/z = 287.2 [M + H]. ¹H NMR (400 MHz, CDCl₃) δ 8.30 (1H, d, J = 8.0 Hz), 7.45 (1H, d, J = 8.0 Hz), 7.25 (2H, m), 6.76 (1H, m), 6.62 (2H, m), 5.10 (2H, s), 3.65 (2H, dt, J = 6.9, 2.5 Hz), 3.20 (2H, t, J = 6.7 Hz), 3.16 (s, 3 H).

2-((3-Fluorophenoxy)methyl)-6-isobutyl-7,8-dihydro-1,6-naphthyridin-5(6H)-one (13d). 2-((3-Fluorophenoxy)methyl)-7,8-dihydro-1,6-naphthyridin-5(6H)-one (13b) (100 mg, 0.41 mmol) was dissolved in DMF (2.0 mL). KOt-Bu (55 mg, 0.5 mmol) was added followed by 1-bromo-2-methylpropane (70 μL, 0.5 mmol). The mixture was heated to 60 °C for 4 h. The mixture was then quenched with H₂O (2.0 mL) and extracted with EtOAc (3×). The organic layers were combined, washed with brine, and concentrated. The resulting crude mixture was purified by RP-HPLC to give title compound as a powder (43 mg, 44%). ¹H NMR (400 MHz, CDCl₃) δ 8.37 (1H, d, J = 8.0 Hz), 7.51 (1H, d, J = 8.0 Hz), 7.22 (1H, m), 6.76 (1H, m), 6.69 (2H, m), 5.19 (2H, s), 3.65 (2H, t, J = 6.8 Hz), 3.40 (2H, d, J = 7.5 Hz), 3.19 (2H, t, J = 6.7 Hz), 2.05 (1H, sep, J = 6.8 Hz), 0.97 (6H, d, J = 6.7 Hz). ¹³C NMR (100 MHz, CDCl₃) δ 163.6 (d, J_{C-F} = 244.2 Hz), 163.4, 159.5 (d, J_{C-F} = 10.7 Hz), 159.1, 157.4, 137.1, 130.4 (d, J_{C-F} = 10.0 Hz), 124.5, 119.9, 110.5 (d, J_{C-F} = 2.9 Hz), 108.2 (d, J_{C-F} = 21.2 Hz), 102.7 (d, J_{C-F} = 24.9 Hz), 70.5, 54.7, 45.8, 30.9, 27.2, 20.1. HRMS (ES⁺, M + H) calcd for C₁₉H₂₂FN₂O₂, 329.1665; found, 329.1662.

6-(Cyclopropylmethyl)-2-((3-fluorophenoxy)methyl)-7,8-dihydro-1,6-naphthyridin-5(6H)-one (13e). Starting from 2-((3-fluorophenoxy)methyl)-7,8-dihydro-1,6-naphthyridin-5(6H)-one (13b) (100 mg, 0.41 mmol) and (bromomethyl)cyclopropane (50 μL, 0.50 mmol), the general procedure outlined in 13d was performed. RP-HPLC afforded the title compound as a powder (64 mg, 66%). ¹H

NMR (400 MHz, CDCl₃) δ 8.36 (1H, d, J = 8.0 Hz), 7.50 (1H, d, J = 8.0 Hz), 7.23 (1H, m), 6.75 (1H, m), 6.68 (2H, m), 5.18 (2H, s), 3.75 (2H, t, J = 6.7 Hz), 3.47 (2H, d, J = 7.0 Hz), 3.21 (2H, t, J = 6.7 Hz), 1.07 (1H, m), 0.55 (2H, m), 0.31 (2H, m). ¹³C NMR (100 MHz, CDCl₃) δ 163.6 (d, J_{C-F} = 244.2 Hz), 163.1, 159.5, (d, J_{C-F} = 10.8 Hz), 159.1, 157.5, 137.0, 130.3 (d, J_{C-F} = 9.9 Hz), 124.4, 119.8, 110.5 (d, J_{C-F} = 2.8 Hz), 108.2 (d, J_{C-F} = 21.2 Hz), 102.7 (d, J_{C-F} = 24.8 Hz), 70.5, 51.4, 45.2, 30.8, 9.5, 3.5. HRMS (ES⁺, M + H) calcd for C₁₉H₂₀FN₂O₂, 327.1509; found, 327.1508.

6-(4-Fluorophenyl)-2-(phenoxymethyl)-7,8-dihydro-1,6-naphthyridin-5(6H)-one (13f). 2-(Phenoxymethyl)-7,8-dihydro-1,6-naphthyridin-5(6H)-one (13a, 50 mg, 0.19 mmol), 1-bromo-2,4-difluorobenzene (42 μL, 0.38 mmol), CuI (7.2 mg, 0.038 mmol), and potassium carbonate (52 mg, 0.38 mmol) were combined in a 2.0 mL microwave vial and placed under an argon atmosphere. Degassed toluene was added followed by N¹,N²-dimethylethane-1,2-diamine (12 μL, 0.110 mmol) and the mixture heated at 120 °C for 16 h. The mixture was cooled to rt, filtered over Celite, and the filtrate concentrated to dryness. RP-HPLC purification afforded the title compound as a powder (16 mg, 31%). ¹H NMR (400 MHz, CDCl₃) δ 8.43 (1H, d, J = 8.0 Hz), 7.60 (1H, d, J = 8.0 Hz), 7.33 (4H, m), 7.12 (2H, m), 6.99 (3H, m), 5.25 (2H, m), 4.06 (2H, t, J = 6.7 Hz), 3.36 (2H, t, J = 6.6 Hz). ¹³C NMR (100 MHz, CDCl₃) δ 163.3, 160.9 (d, J_{C-F} = 245.0 Hz), 160.7, 158.1, 157.5, 138.4 (d, J_{C-F} = 3.2 Hz), 137.5, 129.6, 127.0 (d, J_{C-F} = 8.5 Hz), 124.3, 121.4, 120.1, 115.9 (d, J_{C-F} = 22.5 Hz), 114.8, 70.1, 48.7, 31.2. HRMS (ES⁺, M + H) calcd for C₂₁H₁₈FN₂O₂, 349.1352; found, 349.1351.

2-((3-Fluorophenoxy)methyl)-6-(5-fluoropyridin-2-yl)-7,8-dihydro-1,6-naphthyridin-5(6H)-one (13h). 2-((3-Fluorophenoxy)methyl)-7,8-dihydro-1,6-naphthyridin-5(6H)-one (13b, 26 mg, 0.095 mmol), 2-bromo-5-fluoropyridine (33 mg, 0.19 mmol), CuI (3.8 mg, 0.02 mmol), and potassium carbonate (26 mg, 0.19 mmol) were combined in a 2.0 mL microwave vial and placed under an argon atmosphere. Degassed toluene (1.0 mL) was added followed by N¹,N²-dimethylethane-1,2-diamine (5.8 μL, 0.053 mmol) and the mixture heated at 120 °C for 16 h. The mixture was cooled to rt and filtered over Celite. The filtrate was diluted with H₂O and extracted with EtOAc (3×). The organic layers were combined and concentrated to dryness. RP-HPLC purification afforded the title compound as a powder (31 mg, 89%). ¹H NMR (400 MHz, CDCl₃) δ 8.46 (1H, d, J = 8.0 Hz), 8.29 (1H, d, J = 3.0 Hz), 8.01 (1H, dd, J = 9.1, 4.0 Hz), 7.57 (1H, d, J = 8.1 Hz), 7.47 (1H, m), 7.23 (1H, m), 6.77 (1H, m), 6.71 (2H, m), 5.23 (2H, s), 4.38 (2H, t, J = 6.7 Hz), 3.32 (2H, t, J = 6.6 Hz). ¹³C NMR (100 MHz, CDCl₃) δ 163.6 (d, J_{C-F} = 244.4 Hz), 163.6, 160.4, 159.4 (d, J_{C-F} = 10.8 Hz), 158.4, 156.8 (d, J_{C-F} = 252.0 Hz), 149.5 (d, J_{C-F} = 7.8 Hz), 137.6, 135.1 (d, J_{C-F} = 25.2 Hz), 130.4 (d, J_{C-F} = 9.9 Hz), 124.4, 124.3 (d, J_{C-F} = 19.7 Hz), 120.9 (d, J_{C-F} = 4.5 Hz), 119.9, 110.4 (d, J_{C-F} = 2.9 Hz), 108.3 (d, J_{C-F} = 21.1 Hz), 102.7 (d, J_{C-F} = 24.9 Hz), 70.5, 45.0, 31.2. HRMS (ES⁺, M + H) calcd for C₂₀H₁₆F₂N₃O₂, 368.1211; found, 368.1210.

6-Benzyl-2-((3-fluorophenoxy)methyl)-7,8-dihydro-1,6-naphthyridin-5(6H)-one (13i). Starting from 2-((3-fluorophenoxy)methyl)-7,8-dihydro-1,6-naphthyridin-5(6H)-one (13b) (100 mg, 0.41 mmol) and (bromomethyl)benzene (67 μL, 0.55 mmol), the general procedure outlined in 13d was performed. RP-HPLC afforded the title compound as a powder (74 mg, 66%). ¹H NMR (400 MHz, CDCl₃) δ 8.44 (1H, d, J = 8.0 Hz), 7.53 (1H, d, J = 8.0 Hz), 7.32 (5H, m), 7.24 (1H, m), 6.76 (1H, m), 6.69 (2H, m), 5.19 (2H, s), 4.80 (2H, s), 3.59 (2H, t, J = 6.8 Hz), 3.15 (2H, t, J = 6.8 Hz). ¹³C NMR (100 MHz, CDCl₃) δ 163.6 (d, J_{C-F} = 244.3 Hz), 163.4, 159.4 (d, J_{C-F} = 10.6 Hz), 159.3, 157.5, 137.2, 136.9, 130.4 (d, J_{C-F} = 10.0 Hz), 128.8, 128.1, 127.7, 124.2, 119.9, 110.5 (d, J_{C-F} = 2.9 Hz), 108.2 (d, J_{C-F} = 21.4 Hz), 102.7 (d, J_{C-F} = 24.9 Hz), 70.5, 50.4, 44.5, 30.7. HRMS (ES⁺, M + H) calcd for C₂₂H₂₀FN₂O₂, 363.1509; found, 363.1507.

3-Phenoxymethyl-6,7-dihydro-5H-[1,7]naphthyridin-8-one (14a). Ring-closure step: Starting from 3-(2-oxo-ethyl)-5-phenoxymethylpyridine-2-carboxylic acid methyl ester (128 mg, 0.45 mmol) and benzylamine (0.059 mL, 0.54 mmol) in CH₂Cl₂ (8 mL), the mixture was stirred at rt for 1 h and sodium triacetoxyborohydride (95 mg, 0.45 mmol) was added and the mixture was stirred at rt for 16 h. The

mixture was diluted with CH_2Cl_2 and washed with a saturated solution of NaHCO_3 and brine. The organic layer was separated, dried (Na_2SO_4), filtered, and the solvents evaporated in vacuo. The crude product was purified by flash column chromatography (silica; 7N solution of ammonia in methanol in CH_2Cl_2 0/100 to 4/96). The desired fractions were collected and concentrated to yield, 7-benzyl-3-phenoxyethyl-6,7-dihydro-5H-[1,7]naphthyridin-8-one as an oil (41 mg, 23%). LCMS t_R = 2.83 min, > 90% at 215 and 254 nm, m/z = 255.1 [M + H]. Debenzylation step: Trifluoromethanesulfonic acid (0.020 mL, 0.23 mmol) was added to a solution of 7-benzyl-3-phenoxyethyl-6,7-dihydro-5H-[1,7]naphthyridin-8-one (20 mg, 0.058 mmol) in toluene (0.5 mL) in a sealed tube. The mixture was stirred at 150 °C for 15 min under microwave irradiation. DOWEX 1 \times 2–100 (strongly basic anion exchanger) (300 mg) was added, followed by MeOH (1 mL). The mixture was shaken 4 h at rt, and the resin was filtered and washed with CH_2Cl_2 (1 mL), MeOH (1 mL), CH_2Cl_2 (1 mL), and MeOH (1 mL). The filtrate was evaporated in vacuo. The crude product was purified by flash column chromatography (silica; 7 M ammonia in methanol in CH_2Cl_2 0/100 to 5/95). The desired fractions were collected and the solvents evaporated in vacuo to yield an impure fraction which was purified by RP-HPLC on (C18 XBridge 19 mm \times 100 mm 5 μm). Mobile phase (gradient from 80% 0.1% $\text{NH}_4\text{CO}_3\text{H}/\text{NH}_4\text{OH}$ pH 9 solution in water, 20% CH_3CN to 0% 0.1% $\text{NH}_4\text{CO}_3\text{H}/\text{NH}_4\text{OH}$ pH 9 solution in water, 100% CH_3CN) to yield **14a** as a white solid (6.26 mg, 42% yield). LCMS t_R = 1.36 min, > 98% at 215 and 254 nm, m/z = 255.1 [M + H]. ^1H NMR (500 MHz, CDCl_3) δ 8.74 (d, J = 1.4 Hz, 1 H), 7.73 (br. s, 1 H), 7.39–7.29 (m, 2 H), 7.24 (br. s, 1 H), 7.05–6.94 (m, 3 H), 5.14 (s, 2 H), 3.64 (td, J = 6.6, 2.9 Hz, 2 H), 3.09 (t, J = 6.6 Hz, 2 H).

7-Methyl-3-(phenoxyethyl)-6,7-dihydro-1,7-naphthyridin-8(5H)-one (14b). Methylamine (2.0 M in THF) (2 mL) was added to a stirred solution of 3-(2-oxo-ethyl)-5-phenoxyethyl-pyridine-2-carboxylic acid methyl ester (40 mg, 0.14 mmol) in CH_2Cl_2 (2 mL). The mixture was stirred at rt for 1 h. Then, sodium triacetoxyborohydride (45 mg, 0.21 mmol) was added and the mixture was stirred at rt for 16 h. The mixture was diluted with CH_2Cl_2 and washed with a saturated solution of NaHCO_3 and brine. The organic layer was separated, dried (Na_2SO_4), filtered, and the solvents evaporated in vacuo. The crude product was purified by flash column chromatography (silica; 7N solution of ammonia in methanol in CH_2Cl_2 0/100 to 4/96). The desired fractions were collected and the solvents evaporated in vacuo to yield an impure fraction which was repurified by RP-HPLC on (C18 XBridge 19 mm \times mm 100 5 μm). Mobile phase (gradient from 80% 0.1% $\text{NH}_4\text{CO}_3\text{H}/\text{NH}_4\text{OH}$ pH 9 solution in water, 20% CH_3CN to 0% 0.1% $\text{NH}_4\text{CO}_3\text{H}/\text{NH}_4\text{OH}$ pH 9 solution in water, 100% CH_3CN) to yield **14b** as a white solid (5.8 mg, 15%). LCMS t_R = 1.59 min, > 98% at 215 and 254 nm, m/z = 269.1 [M + H]. ^1H NMR (500 MHz, CDCl_3) δ 8.73 (d, J = 1.7 Hz, 1 H), 7.68 (s, 1 H), 7.36–7.28 (m, 2 H), 7.08–6.90 (m, 3 H), 5.13 (s, 2 H), 3.62 (t, J = 6.6 Hz, 2 H), 3.22 (s, 3 H), 3.08 (t, J = 6.8 Hz, 2 H).

3-Phenoxyethyl-7R-(1,2,2-trimethyl-propyl)-6,7-dihydro-5H-[1,7]naphthyridin-8-one (14c). Starting from 3-(2-oxo-ethyl)-5-phenoxyethyl-pyridine-2-carboxylic acid methyl ester (40 mg, 0.14 mmol) and (R)-(+)-3,3-dimethyl 2-aminobutane 0.039 mL, 0.34 mmol following the procedure described for compound **14a–b**, compound **14c** was obtained as a beige solid (24 mg, 25%). LCMS t_R = 2.82 min, > 98% at 215 and 254 nm, m/z = 339.1 [M + H]. ^1H NMR (500 MHz, CDCl_3) δ 8.73 (d, J = 1.7 Hz, 1 H), 7.68 (s, 1 H), 7.28–7.37 (m, 2 H), 6.92–7.04 (m, 3 H), 5.13 (s, 2 H), 4.92 (q, J = 7.2 Hz, 1 H), 3.62–3.46 (m, 2 H), 3.10–2.98 (m, 1 H), 2.98–2.84 (m, 1 H), 1.22 (d, J = 7.2 Hz, 3 H), 1.00 (s, 9 H); α_D^{20} = -15.7° (c = 0.55 w/v%, MeOH).

7-(4-Fluoro-phenyl)-3-phenoxyethyl-6,7-dihydro-5H-[1,7]naphthyridin-8-one (14d). 4-Fluoroaniline (0.032 mL, 0.34 mmol) was added to a stirred solution of 3-(2-oxo-ethyl)-5-phenoxyethyl-pyridine-2-carboxylic acid methyl ester (80 mg, 0.28 mmol) in CH_2Cl_2 (4 mL). The mixture was stirred at rt for 1 h. Then, sodium triacetoxyborohydride (89 mg, 0.42 mmol) was added and the mixture was stirred at rt for 16 h. Then, acetic acid (0.040 mL) was added and the mixture was stirred at rt for additional 20 h. The mixture was

diluted with CH_2Cl_2 and washed with a saturated solution of NaHCO_3 and brine. The organic layer was separated, dried (Na_2SO_4), filtered, and the solvents evaporated in vacuo. The crude product was purified by flash column chromatography (silica; 7N solution of ammonia in methanol in CH_2Cl_2 0/100 to 4/96). The desired fractions were collected and the solvents evaporated in vacuo to yield an impure fraction which was repurified by RP-HPLC on (C18 XBridge 19 mm \times 100 mm, 5 μm). Mobile phase (gradient from 80% 0.1% $\text{NH}_4\text{CO}_3\text{H}/\text{NH}_4\text{OH}$ pH 9 solution in water, 20% CH_3CN to 0% 0.1% $\text{NH}_4\text{CO}_3\text{H}/\text{NH}_4\text{OH}$ pH 9 solution in water, 100% CH_3CN), to yield **14d** as a white solid (15 mg, 15%). LCMS t_R = 2.00 min, > 98% at 215 and 254 nm, m/z = 349.1 [M + H]. ^1H NMR (500 MHz, CDCl_3) δ 8.78 (d, J = 1.7 Hz, 1 H), 7.76 (br. s, 1 H), 7.42–7.36 (m, 2 H), 7.35–7.29 (m, 2 H), 7.16–7.07 (m, 2 H), 7.01 (t, J = 7.5 Hz, 1 H), 6.98 (d, J = 7.8 Hz, 2 H), 5.17 (s, 2 H), 4.01 (t, J = 6.4 Hz, 2 H), 3.22 (t, J = 6.4 Hz, 2 H).

6-Phenoxyethyl-3,4-dihydro-2H-[2,7]naphthyridin-1-one (15a). A 7N solution of ammonia in methanol (5.5 mL) was added to 6-phenoxyethyl-4-vinyl-nicotinic acid methyl ester (**33**, 55 mg, 0.2 mmol). The mixture was stirred at 100 °C for 16 h. The solvents were evaporated in vacuo. The crude product was purified by flash chromatography (silica; AcOEt in CH_2Cl_2 0/100 to 100/0). The desired fractions were collected and the solvents evaporated in vacuo to yield an impure fraction which was triturated with Et₂O and repurified by RP-HPLC on (C18 XBridge 30 mm \times 100 mm, 5 μm). Mobile phase (gradient from 80% 0.1% $\text{NH}_4\text{CO}_3\text{H}/\text{NH}_4\text{OH}$ pH 9 solution in water, 20% CH_3CN to 0% 0.1% $\text{NH}_4\text{CO}_3\text{H}/\text{NH}_4\text{OH}$ pH 9 solution in water, 100% CH_3CN) to yield **15a** as a white solid (20 mg, 39%); mp 193 °C. LCMS t_R = 1.47 min, > 98% at 215 and 254 nm, m/z = 255.1 [M + H]. ^1H NMR (400 MHz, CDCl_3) δ 9.18 (s, 1 H), 7.43 (d, J = 0.5 Hz, 1 H), 7.36–7.28 (m, 2 H), 7.06–6.94 (m, 3 H), 6.26 (br s, 1 H), 5.24 (s, 2 H), 3.61 (td, J = 6.6, 2.9 Hz, 2 H), 3.03 (t, J = 6.7 Hz, 2 H).

2-Methyl-6-phenoxyethyl-3,4-dihydro-2H-[2,7]naphthyridin-1-one (15b). Starting from 6-phenoxyethyl-4-vinyl-nicotinic acid methyl ester (**33**, 55 mg, 0.2 mmol) and 2 M methylamine in THF (5.5 mL) following the procedure described for compound **15a**, compound **15b** was obtained as a white solid (51 mg, 93%); mp 134 °C. LCMS t_R = 1.72 min, > 98% at 215 and 254 nm, m/z = 269.1 [M + H]. ^1H NMR (500 MHz, CDCl_3) δ 9.18 (s, 1 H), 7.38 (s, 1 H), 7.31 (s, 2 H), 7.04–6.95 (m, 3 H), 5.23 (s, 2 H), 3.59 (t, J = 6.6 Hz, 2 H), 3.16 (s, 3 H), 3.03 (t, J = 6.6 Hz, 2 H).

6-Phenoxyethyl-2(R)-(1,2,2-trimethyl-propyl)-3,4-dihydro-2H-[2,7]naphthyridin-1-one (15c). Acetic acid (0.006 mL, 0.11 mmol) was added to a solution of 6-phenoxyethyl-4-vinyl-nicotinic acid methyl ester (**33**, 29 mg, 0.11 mmol) and (R)-(+)-3,3-dimethyl 2-aminobutane (0.030 mL, 0.225 mmol) in MeOH (1 mL). The mixture was stirred at 100 °C for 16 h. Then (R)-(+)-3,3-dimethyl 2-aminobutane (0.030 mL, 0.225 mmol) and acetic acid (0.006 mL, 0.11 mmol) were added, and the mixture was heated at 100 °C for 2 days. The solvents were evaporated in vacuo and the residue diluted with CH_2Cl_2 and extracted with a saturated solution of NaHCO_3 . The organic layer was separated, dried (Na_2SO_4), filtered, and the solvents evaporated in vacuo. The crude product was purified by flash chromatography (silica; AcOEt in CH_2Cl_2 0/100 to 30/70). The desired fractions were collected and the solvents evaporated in vacuo to yield compound **15c** as a colorless oil which solidified upon standing at room temperature (29 mg, 79%). LCMS t_R = 3.10 min, > 98% at 215 and 254 nm, m/z = 339.1 [M + H]. ^1H NMR (500 MHz, CDCl_3) δ 9.19 (s, 1 H), 7.38 (s, 1 H), 7.31 (t, J = 8.1 Hz, 2 H), 7.03–6.92 (m, 3 H), 5.24 (s, 2 H), 4.83 (q, J = 7.2 Hz, 1 H), 3.59–3.43 (m, 2 H), 3.06–2.93 (m, 1 H), 2.93–2.81 (m, 1 H), 1.21 (d, J = 6.9 Hz, 3 H), 0.99 (s, 9 H).

2-(4-Fluoro-phenyl)-6-phenoxyethyl-3,4-dihydro-2H-[2,7]naphthyridin-1-one (15d). Starting from 6-phenoxyethyl-4-vinyl-nicotinic acid methyl ester (**33**, 30 mg, 0.11 mmol) and 4-fluoroaniline (0.044 mL, 0.47 mmol) following the procedure described for compound **15c**, title compound **15d** was obtained as a white solid (24 mg, 62%); mp 198.8 °C. LCMS t_R = 2.66 min, > 98% at 215 and 254 nm, m/z = 349.1 [M + H]. ^1H NMR (500 MHz, CDCl_3) δ 9.24 (s, 1

H), 7.46 (s, 1 H), 7.39–7.29 (m, 4 H), 7.17–7.08 (m, 2 H), 7.04–6.96 (m, 3 H), 5.27 (s, 2 H), 3.99 (t, $J = 6.5$ Hz, 2 H), 3.17 (t, $J = 6.4$ Hz, 2 H).

Cyclopropyl(3-((3-fluorobenzyl)oxy)-7,8-dihydro-1,6-naphthyridin-6(5H)-yl)methanone (20d). 3-(3-Bromo-7,8-dihydro-1,6-naphthyridin-6(5H)-yl)(cyclopropyl)methanone (35a, 35 mg, 0.125 mmol), 3-fluorobenzyl alcohol (15 mg, 0.125 mmol), cesium carbonate (59 mg, 0.18 mmol), CuI (3 mg, 0.01 mmol), and 1,10-phenanthroline (3.9 mg, 0.02 mmol) were combined in a 2.0 mL microwave vial and placed under an argon atmosphere. Degassed toluene was added and the mixture heated at 110 °C for 4 h. The mixture was cooled to rt, filtered over Celite, and the filtrate concentrated to dryness. RP-HPLC purification afforded **20d** as an off-white powder (15 mg, 33%). LCMS $t_R = 0.79$ min, > 98% at 215 and 254 nm, $m/z = 328.1$ [M + H]. HRMS (ES+, M + H) calcd for $C_{22}H_{20}FN_2O_2$, 327.1509; found, 327.1512.

(3-(Benzyloxy)-7,8-dihydro-1,6-naphthyridin-6(5H)-yl)(4-fluorophenyl)methanone (20g). 3-Bromo-7,8-dihydro-1,6-naphthyridin-6(5H)-yl(4-fluorophenyl)methanone (35c, 28 mg, 0.09 mmol), benzyl alcohol (9.6 mg, 0.09 mmol), cesium carbonate (43 mg, 0.13 mmol), CuI (2 mg, 0.009 mmol), and 1,10-phenanthroline (3.2 mg, 0.018 mmol) were combined in a 2.0 mL microwave vial and placed under an argon atmosphere. Degassed toluene was added and the mixture heated at 110 °C for 4 h. The mixture was cooled to rt, filtered over Celite, and the filtrate concentrated to dryness. RP-HPLC purification afforded the **20g** as an off-white powder (6.9 mg, 22%). LCMS $t_R = 0.85$ min, > 98% at 215 and 254 nm, $m/z = 363.1$ [M + H]. HRMS (ES+, M + H) calcd for $C_{22}H_{22}FN_2O_2$, 363.1509; found, 363.1503.

(4-Fluorophenyl)(3-(phenoxymethyl)-7,8-dihydro-1,6-naphthyridin-6(5H)-yl)methanone (20a). (4-Fluorophenyl)(3-(hydroxymethyl)-7,8-dihydro-1,6-naphthyridin-6(5H)-yl)methanone (39, 40 mg, 0.14 mmol), phenol (40 mg, 0.43 mmol), and polystyrene supported triphenylphosphine (150 mg, 0.45 mmol) were combined in THF (6 mL) and diisopropyl azodicarboxylate (42 mg, 0.21 mmol) was added, and the reaction was allowed to stir overnight at rt. The reaction mixture was filtered through Celite and concentrated in vacuo. The residue was purified via RP-HPLC (10–90% gradient of CH_3CN in water with 0.1% TFA modifier) to afford title compound as an off-white powder (35 mg, 69%). LCMS $t_R = 0.75$ min, > 98% at 215 and 254 nm, $m/z = 363.1$ [M + H]. 1H NMR (400 MHz, $CDCl_3$) δ 8.77 (s, 1H), 8.06 (s, 1H), 7.53–7.49 (m, 3H), 7.36 (t, $J = 8.0$, 2H), 7.18 (t, $J = 8.0$, 2H), 7.06 (t, $J = 8.2$, 1H), 6.87 (d, $J = 8.0$, 1H), 5.18 (s, 2H), 4.98 (s, 2H), 3.92 (s, 2H), 3.36 (t, $J = 6.0$, 2H). HRMS (ES+, M + H) calcd for $C_{22}H_{19}FN_2O_2$, 362.1431; found, 362.1434.

Fluorescence-Based Calcium Flux Assays (Concentration–Response Curves (Potency) and Glutamate Fold Shifts (Efficacy)). For measurement of compound-evoked increases in intracellular calcium, HEK293 cells stably expressing rat mGlu₅ were plated in 384-well,⁴⁴ poly-D-lysine coated, black-walled, clear-bottomed plates in 20 μ L of assay medium (DMEM supplemented with 10% dialyzed fetal bovine serum, 20 mM HEPES, and 1 mM sodium pyruvate) at a density of 15000 cells/well. Cells were grown overnight at 37 °C/5% CO₂. The next day, medium was removed and cells were incubated with 20 μ L/well of 1 μ M Fluo-4AM (Invitrogen, Carlsbad, California) prepared as a 2.3 mM stock in dimethyl sulfoxide (DMSO) and mixed in a 1:1 ratio with 10% (w/v) pluronic acid F-127 and diluted in calcium assay buffer (Hank's Balanced Salt Solution (HBSS; Invitrogen, Carlsbad, CA) supplemented with 20 mM HEPES and 2.5 mM probenecid, pH 7.4) for 50 min at 37 °C. Dye loading solution was then removed and replaced with 20 μ L/well of assay buffer. For PAM potency curves, mGlu₅ compounds were diluted in calcium assay buffer and added to the cells, followed by the addition of an EC₂₀ concentration of glutamate 140 s later and then an EC₈₀ concentration of glutamate 90–120 s later. For fold-shift experiments, either a single concentration (10 μ M) or multiple fixed concentrations (55 nM to 30 μ M) of mGlu₅ compound or vehicle was added, followed by the addition of a concentration–response curve (CRC) of glutamate 140 s later. Calcium flux was measured over time as an increase in fluorescence using a Functional Drug Screening System 6000 (FDSS

6000, Hamamatsu, Japan). The change in relative fluorescence over basal was calculated before normalization to the maximal response to glutamate. A 2-fold enhancement over basal response at the maximum concentration was sufficient criteria for weak PAM activity (e.g., 40% Glu max at an EC₂₀ add of glutamate; the basal EC₂₀ response range allowed was 10–30%).

Selectivity Screening. mGlu₇. To assess the effect of test compounds at mGlu₇, Ca²⁺ mobilization assays were performed as described previously.^{46,47} Briefly, HEK293 cells stably expressing rat mGlu₇ were plated in black-walled, clear-bottomed, poly-D-lysine coated 384-well plates (Greiner Bio-One, Monroe, NC) in assay medium at a density of 20000 cells/well. Calcium flux was measured over time as an increase in fluorescence of the Ca²⁺ indicator dye, Fluo-4AM using a FDSS 6000. Either vehicle or a fixed concentration of test compound (10 μ M, final concentration) was added, followed 140 s later by a CRC of glutamate. Data were analyzed as described above.

Group II and Group III mGlu_s. The functional activity of the compounds of interest was assessed at the rat group II and III mGlu receptors by measuring thallium flux through GIRK channels as previously described.⁶² Briefly, HEK293-GIRK cells expressing mGlu subtypes 2, 3, 4, 6, 7, or 8 were plated into 384-well, black-walled, clear-bottom poly-D-lysine coated plates at a density of 15000 cells/well in assay medium. A single concentration of test compound (10 μ M) or vehicle was added, followed 140 s later by a CRC of glutamate (or L-AP4 for mGlu₇) diluted in thallium buffer (125 mM NaHCO₃, 1 mM MgSO₄, 1.8 mM CaSO₄, 5 mM glucose, 12 mM thallium sulfate, 10 mM HEPES), and fluorescence was measured using a FDSS 6000. Data were analyzed as described previously.⁶²

In Vivo Pharmacology. Animal Husbandry. Animals were housed in the animal care facility certified by the American Association for the Accreditation of Laboratory Animal Care (AAALAC) under a 12 h light/dark cycle (lights on, 7 a.m.; lights off, 7 p.m.) and had free access to food and water. The animals used in these experiments were food-deprived the evening before experimentation for oral administration of test compound. The experimental protocols performed during the light cycle were approved by the Institutional Animals Care and Use Committee of Vanderbilt University and conformed to the guidelines established by the National Research Council Guide for the Care and Use of Laboratory Animals.

Preparation of Test Article. **12c** was formulated in volumes specific to the number of animals dosed each day. The solutions were formulated so that animals were injected with a maximal dosing volume of 10 mL/kg. The appropriate amount according to the dosage was mixed into a 20% 2-(hydroxypropyl)- β -cyclodextrin in sterile water (HP- β -CD; Sigma, catalogue no. C0926-10G) solution. Each mixture was ultrahomogenized on ice for 2–3 min using a hand-held tissue homogenizer. Next, the pH of all solutions was checked using 0–14 EMD pH strips and adjusted to a pH of 6–7 if necessary with 1N NaOH. The mixtures were then vortexed and stored in a sonication bath at 40 °C until time of injection. *d*-Amphetamine hemisulfate (AMP) was obtained from Sigma (catalogue no. A5880-1G; St. Louis, MO). Salt-correction was used to determine the correct amount of the *d*-amphetamine hemisulfate form in mg to add to sterile water in order to yield a 1 mg/mL solution, injected with a maximal dosing volume of 10 mL/kg.

Reversal of Amphetamine-Induced Hyperlocomotion. Studies were conducted using Smart Open Field activity chambers (27 cm \times 27 cm \times 20 cm) (Kinder Scientific, Poway, CA) equipped with 16 horizontal (*x*- and *y*-axes) infrared photobeams. Changes in locomotor activity were measured as the number of photobeam breaks over time and were recorded with a Pentium I computer equipped with rat activity monitoring system software (Motor Monitor, Kinder Scientific, Poway, CA). Male Harlan Sprague–Dawley rats (Harlan Laboratories, Indianapolis, IN) weighing 250–375 g were used. Animals were habituated in the locomotor activity test chambers for 30 min. Animals were next pretreated for an additional 30 min with either vehicle or a dose of **12c** po, followed by a subcutaneous injection of 1 mg/kg amphetamine or vehicle and monitored for an additional 60 min.

Treatment Groups. Dose group 1, VAMP = 20% β -CD (12c vehicle), po + 1 mg/kg AMP, sc ($n = 8$). Dose group 2, 3AMP = 3 mg/kg 12c, po + 1 mg/kg AMP, sc ($n = 6$). Dose group 3, 10AMP = 10 mg/kg 12c, po + 1 mg/kg AMP, sc ($n = 7$). Dose group 4, 30AMP = 30 mg/kg 12c, po + 1 mg/kg AMP, sc ($n = 8$). Dose group 5, 56.6AMP = 56.6 mg/kg 12c, po + 1 mg/kg AMP, sc ($n = 8$). Dose group 6, 100AMP = 100 mg/kg 12c, po + 1 mg/kg AMP, sc ($n = 8$). Dose group 7, 100V = 100 mg/kg 12c, po + sterile water (AMP vehicle), sc ($n = 8$). Changes in locomotor activity were recorded for a total of 120 min. Data were expressed as changes in ambulation defined as the total number of photobeam breaks per 5 min interval. At the end of this behavioral study, each animal was euthanized, then decapitated, and the plasma and brain tissues were collected for the evaluation of exposure levels of 12c.

Data Analysis. Behavioral data were analyzed using a one-way ANOVA with main effects of treatment and time. Post hoc analyses were performed using a Dunnett's t -test with all treatment groups compared to the VAMP group using JMP 8.0 (SAS Institute, Cary, NC) statistical software. Data were graphed using SigmaPlot for Windows version 11.0 (Saugua, MA). A probability of $p \leq 0.05$ was taken as the level of statistical significance. Percent effect and reversal calculations for the 3AMP, 10AMP, 30AMP, 56.6AMP, and 100AMP treatment groups were performed with the following formula relative to the VAMP treatment group: (1) Total number of photobeam breaks in the time interval from $t = 60$ to $t = 120$ was calculated for each rat in each treatment group, (2) mean total number of photobeam breaks in the time interval from $t = 60$ to $t = 120$ was calculated for the VAMP group, (3) percent effect = ratio of the total number of photobeam breaks for each rat in each treatment group divided by the mean total number of photobeam breaks in the time interval from $t = 60$ to $t = 120$ of the VAMP group multiplied by 100, (4) percent reversal = $100 -$ the percent effect for each rat in each treatment group, (5) finally, the mean \pm SE percent reversal for each treatment group was calculated from the individual percent reversal values. Percent effect and change calculations for the VAMP and 100 V treatment groups relative to the VV treatment group were also performed with the following formula: (1) total number of photobeam breaks in the time interval from $t = 60$ to $t = 120$ was calculated for each rat in each treatment group, (2) mean total number of photobeam breaks in the time interval from $t = 60$ to $t = 120$ was calculated for the VV group; (3) percent effect = ratio of the total number of photobeam breaks for each rat in each treatment group divided by the mean total number of photobeam breaks in the time interval from $t = 60$ to $t = 120$ of the VV group multiplied by 100, (4) percent change = the percent effect for each rat in each treatment group $- 100$, (5) finally, the mean \pm SE percent change for each treatment group was calculated from the individual percent change values.

LC-MS/MS Sample Preparation and Analysis Methodology. Brain samples were homogenized in 3 mL of 70:30 2-propanol:water and then centrifuged at 3500 rpm for 5 min. Resulting brain sample supernatant and plasma samples were transferred into a 96-well plate containing plasma blanks, plasma double blank, a standard curve of the test article, and quality control samples for subsequent LC-MS/MS analysis. Each sample was diluted with acetonitrile containing 50 nM carbamazepine (internal standard), centrifuged at 3500 rpm, and the resulting supernatant was transferred to a new 96-well plate. After an equal volume of water was added to each sample (to provide 50:50 acetonitrile:water solution), the plate was analyzed via ESI on a triple-quadrupole mass spectrometer (AB Sciex API-4000) coupled with an autosampling liquid chromatography system (Shimadzu LC-10AD pumps, Leap Technologies CTC PAL autosampler). Analyte (test article) was separated by gradient elution using a C18 3.0 mm \times 50 mm, 3 μ m column (Fortis Technologies) thermostated at 40 $^{\circ}$ C. HPLC mobile phase A was 0.1% formic acid in water (pH unadjusted), mobile phase B was 0.1% formic acid in acetonitrile (pH unadjusted), and the gradient used was 30–90% mobile phase B with 0.2 min hold at 30% B, linear increase to 90% B over 0.8 min, hold at 90% B for 0.6 min, and a return to 30% B over 0.1 min followed by a re-equilibration (0.5 min) to provide a 2.0 min total run

time per sample. HPLC flow rate was 0.5 mL/min, source temperature was 500 $^{\circ}$ C, and mass spectral analyses were performed using the following MRM transitions: 353.5 \rightarrow 259.2 and 353.5 \rightarrow 123.2 m/z . ESI was achieved by a turbo-ion-spray source in positive ionization mode (5.0 kV spray voltage). The raw plasma and brain concentration data obtained by LC-MS/MS were analyzed by Analyst software (AB Sciex, version 1.5.1), which used the ratio of peak area responses of drug relative to internal standard to construct a standard curve with a dynamic range covering the concentrations found in the samples. Free plasma and brain concentrations were calculated by multiplication of the total concentration values by $f_{u,plasma}$ and $f_{u,brain}$, respectively, based on data from in vitro rat plasma protein and rat brain homogenate binding experiments.

Rotarod. The effects of 12c on motor performance were evaluated using an automated rotarod setup with a rotarod (7.0 cm in diameter) rotating at a constant speed of 20 rotations/min (MedAssociates, Inc., St Albans, CA). Male Harlan Sprague–Dawley rats (Harlan Laboratories, Indianapolis, IN) weighing 250–300 g were used. Animals were given two training trials of 120 s on the rotarod with a 10 min interval between trials, followed by baseline assessment of performance with a 120 s trial, and any animals that did not reach a performance criteria of 85 s were excluded from the study. Animals were next pretreated for 30 min with vehicle (20% HP- β -CD) or a dose of 12c ($n = 6$ each group) and then tested on the rotarod using a 120 s trial. The amount of time in seconds that each animal remained on the rotarod was recorded; animals not falling off of the rotarod were given a maximal score of 120 s. Data were expressed as the mean latency to fall off the rotarod in seconds for each treatment group.

Data Analysis. Behavioral data were analyzed using a one-way ANOVA with main effects of treatment. Post hoc analyses were performed using a Dunnett's t test with all treatment groups compared to the vehicle group using JMP 8.0 (SAS Institute, Cary, NC) statistical software. Data were graphed using SigmaPlot for Windows Version 11.0 (Saugua, MA). A probability of $p \leq 0.05$ was taken as the level of statistical significance.

Modified Irwin Neurological Test Battery. Male Harlan Sprague–Dawley rats (Harlan Laboratories, Indianapolis, IN) weighing 250–300 g were used. Animals were evaluated in the modified Irwin neurological test battery at $t = 0$ to provide a baseline measurement across each functional end point. Animals were next administered either vehicle (20% HP- β -CD) or a 100 mg/kg po dose of 12c ($n = 6$ each group) and then assessed after a 30 min, 1 h, and 4 h pretreatment interval in the modified Irwin neurological test battery. Changes in the different functional end points of the Irwin test battery were given a score of 0, 1 or 2, with 0 = no effect, 1 = moderate effect, and 2 = robust full effect. All data were collected blinded to treatment for each animal. The following functional end points were scored. Autonomic nervous system functions: ptosis, exophthalmos, miosis, mydriasis, corneal reflex, pinna reflex, piloerection, respiratory rate, writhing, tail erection, lacrimation, salivation, vasodilation, skin color, irritability, and rectal temperature. Somatomotor nervous system functions: motor activity, ataxia, arch/roll, tremors, leg weakness, rigid stance, spraddle, placing loss, grasping loss, righting loss, catalepsy, tail pinch reaction, escape loss, and physical appearance.

Data Analysis. Mean change values for each functional end point in the Irwin test battery of each treatment group were calculated using Microsoft Excel. Behavioral data were then analyzed using a one-way ANOVA with main effect of treatment. Post hoc analyses were performed using a Dunnett's t test with all treatment groups compared to the vehicle group using JMP 8.0 (SAS Institute, Cary, NC) statistical software. Data were graphed using SigmaPlot for Windows version 11.0 (Saugua, MA). A probability of $p \leq 0.05$ was taken as the level of statistical significance.

■ ASSOCIATED CONTENT

Supporting Information

mGlu selectivity for 12c, 13g, and 14d; operational model affinity and cooperativity calculations (12c), DMPK procedures and methods, rotarod, modified Irwin, Eurofins ancillary

pharmacology, compound characterization, NMR spectra for representative compounds, and subseries 19. This material is available free of charge via the Internet at <http://pubs.acs.org>.

AUTHOR INFORMATION

Corresponding Author

*Phone: (615)-936-8407. Fax: (615)-343-3088. E-mail: shaun.stauffer@vanderbilt.edu. Address: Vanderbilt University Medical Center, Vanderbilt Center for Neuroscience Drug Discovery, 1205 Light Hall, Nashville, Tennessee 37232-0697, United States.

Notes

The authors declare no competing financial interest.

ACKNOWLEDGMENTS

Vanderbilt Center for Neuroscience Drug Discovery (VCNDD) research was supported by grants from Janssen Pharmaceutical Companies of Johnson & Johnson and in part by the NIH (NS031373, MH062646).

ABBREVIATIONS USED

mGlu, metabotropic glutamate receptor; PAM, positive allosteric modulator; NAM, negative allosteric modulator; LTD, long-term depression; MPEP, 2-methyl-6-(phenylethynyl)pyridine; CPPHA, *N*-(4-chloro-2-((1,3-dioxoisindolin-2-yl)methyl)phenyl)-2-hydroxybenzamide; CDPBP, 3-cyano-*N*-(1,3-diphenyl-1*H*-pyrazol-5-yl)benzamide; AHL, amphetamine-induced hyperlocomotion

REFERENCES

- (1) Meltzer, H. Y. Treatment of schizophrenia and spectrum disorders: pharmacotherapy, psychosocial treatments, and neurotransmitter interactions. *Biol. Psychiatry* **1999**, *46*, 1321–1327.
- (2) Lewis, D. A.; Lieberman, J. A. Catching up on schizophrenia: natural history and neurobiology. *Neuron* **2000**, *28*, 325–334.
- (3) Lieberman, J. A.; Stroup, T. S.; McEvoy, J. P.; Swartz, M. S.; Rosenheck, R. A.; Perkins, D. O.; Keefe, R. S.; Davis, S. M.; Davis, C. E.; Lebowitz, B. D.; Severe, J.; Hsiao, J. K. Effectiveness of antipsychotic drugs in patients with chronic schizophrenia. *N. Engl. J. Med.* **2005**, *353*, 1209–1223.
- (4) Nuechterlein, K. H.; Barch, D. M.; Gold, J. M.; Goldberg, T. E.; Green, M. F.; Heaton, R. K. Identification of separable cognitive factors in schizophrenia. *Schizophrenia Res.* **2004**, *72*, 29–39.
- (5) Toda, M.; Abi-Dargham, A. Dopamine hypothesis of schizophrenia: making sense of it all. *Curr. Psychiatry Rep.* **2007**, *9*, 329–336.
- (6) Meltzer, H. Y. Suicide and schizophrenia: clozapine and the InterSePT study. International Clozaril/Leponex Suicide Prevention Trial. *J. Clin. Psychiatry* **1999**, *60* (Suppl 12), 47–50.
- (7) Ray, W. A.; Chung, C. P.; Murray, K. T.; Hall, K.; Stein, C. M. Atypical antipsychotic drugs and the risk of sudden cardiac death. *N. Engl. J. Med.* **2009**, *360*, 225–235.
- (8) Bordi, F.; Ugolini, A. Group I metabotropic glutamate receptors: implications for brain diseases. *Prog. Neurobiol.* **1999**, *59*, 55–79.
- (9) Conn, P. J.; Lindsley, C. W.; Jones, C. K. Activation of metabotropic glutamate receptors as a novel approach for the treatment of schizophrenia. *Trends Pharmacol. Sci.* **2009**, *30*, 25–31.
- (10) Chavez-Noriega, L. E.; Schaffhauser, H.; Campbell, U. C. Metabotropic glutamate receptors: potential drug targets for the treatment of schizophrenia. *Curr. Drug Targets: CNS Neurol. Disord.* **2002**, *1*, 261–281.
- (11) Perroy, J.; Raynaud, F.; Homburger, V.; Rousset, M. C.; Telley, L.; Bockaert, J.; Fagni, L. Direct interaction enables cross-talk between ionotropic and group I metabotropic glutamate receptors. *J. Biol. Chem.* **2008**, *283*, 6799–6805.
- (12) Williams, D. L., Jr.; Lindsley, C. W. Discovery of positive allosteric modulators of metabotropic glutamate receptor subtype 5 (mGluR5). *Curr. Top. Med. Chem.* **2005**, *5*, 825–846.
- (13) Shipe, W. D.; Wolkenberg, S. E.; Williams, D. L., Jr.; Lindsley, C. W. Recent advances in positive allosteric modulators of metabotropic glutamate receptors. *Curr. Opin. Drug Discovery Dev.* **2005**, *8*, 449–457.
- (14) Marino, M. J.; Conn, P. J. Direct and indirect modulation of the *N*-methyl *D*-aspartate receptor. *Curr. Drug Targets: CNS Neurol. Disord.* **2002**, *1*, 1–16.
- (15) Stauffer, S. R. Progress toward positive allosteric modulators of the metabotropic glutamate receptor subtype 5 (mGluR5). *ACS Chem. Neurosci.* **2011**, *2*, 450–470.
- (16) Lindsley, C. W.; Stauffer, S. R. Metabotropic glutamate receptor 5-positive allosteric modulators for the treatment of schizophrenia (2004–2012). *Pharm. Pat. Analyst* **2013**, *2*, 93–108.
- (17) Kinney, G. G.; O'Brien, J. A.; Lemaire, W.; Burno, M.; Bickel, D. J.; Clements, M. K.; Chen, T. B.; Wisnoski, D. D.; Lindsley, C. W.; Tiller, P. R.; Smith, S.; Jacobson, M. A.; Sur, C.; Duggan, M. E.; Pettibone, D. J.; Conn, P. J.; Williams, D. L., Jr. A novel selective positive allosteric modulator of metabotropic glutamate receptor subtype 5 has in vivo activity and antipsychotic-like effects in rat behavioral models. *J. Pharmacol. Exp. Ther.* **2005**, *313*, 199–206.
- (18) Le Poul, E.; Bessis, A. S.; Lutgens, R.; Bonnet, B.; Rocher, J. P.; Epping-Jordan, M. P.; Mutel, V. In vitro pharmacological characterization of selective mGluR5 positive allosteric modulators. 5th International Metabotropic Glutamate Receptors Meeting, Taormina, Italy, 2005.
- (19) Bessis, A.-S.; Bonnet, B.; Le, P. E.; Rocher, J.-P.; Epping-Jordan, M. Preparation of piperidine derivatives as modulators of metabotropic glutamate receptors (mGluR5). WO 2005044797, 2005.
- (20) Sharma, S.; Kedrowski, J.; Rook, J. M.; Smith, R. L.; Jones, C. K.; Rodriguez, A. L.; Conn, P. J.; Lindsley, C. W. Discovery of molecular switches that modulate modes of metabotropic glutamate receptor subtype 5 (mGluR5) pharmacology in vitro and in vivo within a series of functionalized, regioisomeric 2- and 5-(phenylethynyl)pyrimidines. *J. Med. Chem.* **2009**, *52*, 4103–4106.
- (21) Rodriguez, A. L.; Grier, M. D.; Jones, C. K.; Herman, E. J.; Kane, A. S.; Smith, R. L.; Williams, R.; Zhou, Y.; Marlo, J. E.; Days, E. L.; Blatt, T. N.; Jadhav, S.; Menon, U. N.; Vinson, P. N.; Rook, J. M.; Stauffer, S. R.; Niswender, C. M.; Lindsley, C. W.; Weaver, C. D.; Conn, P. J. Discovery of novel allosteric modulators of metabotropic glutamate receptor subtype 5 reveals chemical and functional diversity and in vivo activity in rat behavioral models of anxiolytic and antipsychotic activity. *Mol. Pharmacol.* **2010**, *78*, 1105–1123.
- (22) Gastambide, F.; Cotel, M. C.; Gilmour, G.; O'Neill, M. J.; Robbins, T. W.; Tricklebank, M. D. Selective remediation of reversal learning deficits in the neurodevelopmental MAM model of schizophrenia by a novel mGluR5 positive allosteric modulator. *Neuropsychopharmacology* **2012**, *37*, 1057–1066.
- (23) Gilmour, G.; Broad, L. M.; Wafford, K. A.; Britton, T.; Colvin, E. M.; Fivush, A.; Gastambide, F.; Getman, B.; Heinz, B. A.; McCarthy, A. P.; Prieto, L.; Shanks, E.; Smith, J. W.; Taboada, L.; Edgar, D. M.; Tricklebank, M. D. In vitro characterisation of the novel positive allosteric modulators of the mGlu(5) receptor, LSN2463359 and LSN2814617, and their effects on sleep architecture and operant responding in the rat. *Neuropharmacology* **2013**, *64*, 224–239.
- (24) Zhou, Y.; Manka, J. T.; Rodriguez, A. L.; Weaver, C. D.; Days, E. L.; Vinson, P. N.; Jadhav, S.; Hermann, E. J.; Jones, C. K.; Conn, P. J.; Lindsley, C. W.; Stauffer, S. R. Discovery of *N*-aryl piperazines as selective mGluR5 potentiators with improved in vivo utility. *ACS Med. Chem. Lett.* **2010**, *1*, 433–438.
- (25) Spear, N.; Gadiant, R. A.; Wilkins, D. E.; Do, M.; Smith, J. S.; Zeller, K. L.; Schroeder, P.; Zhang, M.; Arora, J.; Chhajlani, V. Preclinical profile of a novel metabotropic glutamate receptor 5 positive allosteric modulator. *Eur. J. Pharmacol.* **2011**, *659*, 146–154.
- (26) Manka, J. T.; Vinson, P. N.; Gregory, K. J.; Zhou, Y.; Williams, R.; Gogi, K.; Days, E.; Jadhav, S.; Herman, E. J.; Lavreysen, H.; Mackie, C.; Bartolome, J. M.; Macdonald, G. J.; Steckler, T.; Daniels, J.

- S.; Weaver, C. D.; Niswender, C. M.; Jones, C. K.; Conn, P. J.; Lindsley, C. W.; Stauffer, S. R. Optimization of an ether series of mGlu5 positive allosteric modulators: molecular determinants of MPEP-site interaction crossover. *Bioorg. Med. Chem. Lett.* **2012**, *22*, 6481–6185.
- (27) Parmentier-Batteur, S.; Obrien, J. A.; Doran, S.; Nguyen, S. J.; Flick, R. B.; Uslaner, J. M.; Chen, H.; Finger, E. N.; Williams, T. M.; Jacobson, M. A.; Hutson, P. H. Differential effects of the mGluR5 positive allosteric modulator CDPPB in the cortex and striatum following repeated administration. *Neuropharmacology* **2012**, *62*, 1453–1460.
- (28) Rook, J. M.; Noetzel, M. J.; Pouliot, W. A.; Bridges, T. M.; Vinson, P. N.; Cho, H. P.; Zhou, Y.; Gogliotti, R. D.; Manka, J. T.; Gregory, K. J.; Stauffer, S. R.; Dudek, F. E.; Xiang, Z.; Niswender, C. M.; Daniels, J. S.; Jones, C. K.; Lindsley, C. W.; Conn, P. J. Unique signaling profiles of positive allosteric modulators of metabotropic glutamate receptor subtype 5 determine differences in in vivo activity. *Biol. Psychiatry* **2013**, *73*, S01–S09.
- (29) Bridges, T. M.; Rook, J. M.; Noetzel, M. J.; Morrison, R. D.; Zhou, Y.; Gogliotti, R. D.; Vinson, P. N.; Xiang, Z.; Jones, C. K.; Niswender, C. M.; Lindsley, C. W.; Stauffer, S. R.; Conn, P. J.; Daniels, J. S. Biotransformation of a novel positive allosteric modulator of metabotropic glutamate receptor subtype 5 contributes to seizure-like adverse events in rats involving a receptor agonism-dependent mechanism. *Drug Metab. Dispos.* **2013**, *41*, 1703–1714.
- (30) Turlington, M.; Noetzel, M. J.; Chun, A.; Zhou, Y.; Gogliotti, R. D.; Nguyen, E. D.; Gregory, K. J.; Vinson, P. N.; Rook, J. M.; Gogi, K. K.; Xiang, Z.; Bridges, T. M.; Daniels, J. S.; Jones, C.; Niswender, C. M.; Meiler, J.; Conn, P. J.; Lindsley, C. W.; Stauffer, S. R. Exploration of allosteric agonism structure–activity relationships within an acetylene series of metabotropic glutamate receptor 5 (mGlu) positive allosteric modulators (PAMs): discovery of 5-((3-Fluorophenyl)-ethynyl)-N-(3-methyloxetan-3-yl)picolinamide (ML254). *J. Med. Chem.* **2013**, *56*, 7976–7996.
- (31) Bartolome-Nebreda, J. M.; Conde-Ceide, S.; Delgado, F.; Iturrino, L.; Pastor, J.; Pena, M. A.; Trabanco, A. A.; Tresadern, G.; Wassvik, C. M.; Stauffer, S. R.; Jadhav, S.; Gogi, K.; Vinson, P. N.; Noetzel, M. J.; Days, E.; Weaver, C. D.; Lindsley, C. W.; Niswender, C. M.; Jones, C. K.; Conn, P. J.; Rombouts, F.; Lavreysen, H.; Macdonald, G. J.; Mackie, C.; Steckler, T. Dihydrothiazolopyridone derivatives as a novel family of positive allosteric modulators of the metabotropic glutamate 5 (mGlu5) receptor. *J. Med. Chem.* **2013**, *56*, 7243–7259.
- (32) Williams, R.; Manka, J. T.; Rodriguez, A. L.; Vinson, P. N.; Niswender, C. M.; Weaver, C. D.; Jones, C. K.; Conn, P. J.; Lindsley, C. W.; Stauffer, S. R. Synthesis and SAR of centrally active mGlu(5) positive allosteric modulators based on an aryl acetylenic bicyclic lactam scaffold. *Bioorg. Med. Chem. Lett.* **2011**, *21*, 1350–1353.
- (33) Wood, M. R.; Hopkins, C. R.; Brogan, J. T.; Conn, P. J.; Lindsley, C. W. “Molecular switches” on mGluR allosteric ligands that modulate modes of pharmacology. *Biochemistry* **2011**, *50*, 2403–2410.
- (34) Engers, D. W.; Rodriguez, A. L.; Williams, R.; Hammond, A. S.; Venable, D.; Oluwatola, O.; Sulikowski, G. A.; Conn, P. J.; Lindsley, C. W. Synthesis, SAR and unanticipated pharmacological profiles of analogues of the mGluR5 ago-potentiator ADX-47273. *ChemMedChem* **2009**, *4*, S05–S11.
- (35) Lamb, J. P.; Engers, D. W.; Niswender, C. M.; Rodriguez, A. L.; Venable, D. F.; Conn, J. P.; Lindsley, C. W. Discovery of molecular switches within the ADX-47273 mGlu(5) PAM scaffold that modulate modes of pharmacology to afford potent mGlu(5) NAMs, PAMs and partial antagonists. *Bioorg. Med. Chem. Lett.* **2011**, *21*, 2711–2714.
- (36) Lindsley, C. W.; Wisnoski, D. D.; Leister, W. H.; O'Brien, J. A.; Lemaire, W.; Williams, D. L., Jr.; Burno, M.; Sur, C.; Kinney, G. G.; Pettibone, D. J.; Tiller, P. R.; Smith, S.; Duggan, M. E.; Hartman, G. D.; Conn, P. J.; Huff, J. R. Discovery of positive allosteric modulators for the metabotropic glutamate receptor subtype 5 from a series of N-(1,3-diphenyl-1H-pyrazol-5-yl)benzamides that potentiate receptor function in vivo. *J. Med. Chem.* **2004**, *47*, S825–S828.
- (37) de Paulis, T.; Hemstapat, K.; Chen, Y.; Zhang, Y.; Saleh, S.; Alagille, D.; Baldwin, R. M.; Tamagnan, G. D.; Conn, P. J. Substituent effects of N-(1,3-diphenyl-1H-pyrazol-5-yl)benzamides on positive allosteric modulation of the metabotropic glutamate-5 receptor in rat cortical astrocytes. *J. Med. Chem.* **2006**, *49*, 3332–3344.
- (38) O'Brien, J. A.; Lemaire, W.; Wittmann, M.; Jacobson, M. A.; Ha, S. N.; Wisnoski, D. D.; Lindsley, C. W.; Schaffhauser, H. J.; Rowe, B.; Sur, C.; Duggan, M. E.; Pettibone, D. J.; Conn, P. J.; Williams, D. L., Jr. A novel selective allosteric modulator potentiates the activity of native metabotropic glutamate receptor subtype 5 in rat forebrain. *J. Pharmacol. Exp. Ther.* **2004**, *309*, 568–577.
- (39) Zhao, Z.; Wisnoski, D. D.; O'Brien, J. A.; Lemaire, W.; Williams, D. L., Jr.; Jacobson, M. A.; Wittman, M.; Ha, S. N.; Schaffhauser, H.; Sur, C.; Pettibone, D. J.; Duggan, M. E.; Conn, P. J.; Hartman, G. D.; Lindsley, C. W. Challenges in the development of mGluR5 positive allosteric modulators: the discovery of CPPHA. *Bioorg. Med. Chem. Lett.* **2007**, *17*, 1386–1391.
- (40) Noetzel, M. J.; Gregory, K. J.; Vinson, P. N.; Manka, J. T.; Stauffer, S. R.; Lindsley, C. W.; Niswender, C. M.; Xiang, Z.; Conn, P. J. A novel metabotropic glutamate receptor 5 positive allosteric modulator acts at a unique site and confers stimulus bias to mGlu5 signaling. *Mol. Pharmacol.* **2013**, *83*, 835–847.
- (41) Xiong, H.; Brugel, T. A.; Balestra, M.; Brown, D. G.; Brush, K. A.; Hightower, C.; Hinkley, L.; Hoesch, V.; Kang, J.; Koether, G. M.; McCauley, J. P., Jr.; McLaren, F. M.; Panko, L. M.; Simpson, T. R.; Smith, R. W.; Woods, J. M.; Brockel, B.; Chhajlani, V.; Gadiant, R. A.; Spear, N.; Sygowski, L. A.; Zhang, M.; Arora, J.; Breyse, N.; Wilson, J. M.; Isaac, M.; Slassi, A.; King, M. M. 4-Aryl piperazine and piperidine amides as novel mGluR5 positive allosteric modulators. *Bioorg. Med. Chem. Lett.* **2010**, *20*, 7381–7384.
- (42) Rodriguez, A. L.; Zhou, Y.; Williams, R.; David Weaver, C.; Vinson, P. N.; Dawson, E. S.; Steckler, T.; Lavreysen, H.; Mackie, C.; Bartolome, J. M.; Macdonald, G. J.; Scott Daniels, J.; Niswender, C. M.; Jones, C. K.; Jeffrey Conn, P.; Lindsley, C. W.; Stauffer, S. R. Discovery and SAR of a novel series of non-MPEP site mGlu(5) PAMs based on an aryl glycine sulfonamide scaffold. *Bioorg. Med. Chem. Lett.* **2012**, *22*, 7388–7392.
- (43) Conn, J. P.; Lindsley, C. W.; Stauffer, S. R.; Manka, J.; Jacobs, J.; Zhou, Y.; Bartolome, J. M.; Macdonald, G. J.; Conde-Ceide, S.; Jones, C. K. Preparation of naphthyridinone analogs as mGluR5 positive allosteric modulators. WO2012092530, 2012.
- (44) Conn, J. P.; Lindsley, C. W.; Stauffer, S. R.; Manka, J.; Jacobs, J.; Zhou, Y.; Bartolome, J. M.; Macdonald, G. J.; Conde-Ceide, S.; Dawson, E. Preparation of dihydronaphthyridinyl(organo)methanone analogs as positive allosteric mGluR5 modulators for the treatment of neurologic and psychiatric disorders. U.S. Pat. Appl. 20120178776, 2012.
- (45) Manka, J.; Jacobs, J.; Zhou, Y.; Vinson, P. N.; Jadhav, S.; Herman, E. J.; Lavreysen, H.; Mackie, C.; Bartolome, J. M.; Macdonald, G. J.; Steckler, T.; Daniels, J. S.; Weaver, C.; Niswender, C. M.; Jones, C.; Conn, J. P.; Lindsley, C. W.; Stauffer, S. R. Bicyclic tetrahydronaphthridine and dihydronaphthridinone ethers as positive allosteric modulators of mGlu5. Presented at the 244th ACS National Meeting, Philadelphia, Aug 19–23, 2012, Poster MEDI 190.
- (46) Noetzel, M. J.; Rook, J. M.; Vinson, P. N.; Cho, H. P.; Days, E.; Zhou, Y.; Rodriguez, A. L.; Lavreysen, H.; Stauffer, S. R.; Niswender, C. M.; Xiang, Z.; Daniels, J. S.; Jones, C. K.; Lindsley, C. W.; Weaver, C. D.; Conn, P. J. Functional impact of allosteric agonist activity of selective positive allosteric modulators of metabotropic glutamate receptor subtype 5 in regulating central nervous system function. *Mol. Pharmacol.* **2012**, *81*, 120–133.
- (47) Hammond, A. S.; Rodriguez, A. L.; Townsend, S. D.; Niswender, C. M.; Gregory, K. J.; Lindsley, C. W.; Conn, P. J. Discovery of a novel chemical class of mGlu(5) allosteric ligands with distinct modes of pharmacology. *ACS Chem. Neurosci.* **2010**, *1*, 702–716.
- (48) Varnes, J. G.; Marcus, A. P.; Mauger, R. C.; Throner, S. R.; Hoesch, V.; King, M. M.; Wang, X.; Sygowski, L. A.; Spear, N.; Gadiant, R.; Brown, D. G.; Campbell, J. B. Discovery of novel positive

allosteric modulators of the metabotropic glutamate receptor 5 (mGluR5). *Bioorg. Med. Chem. Lett.* **2011**, *21*, 1402–1406.

(49) Conn, J. P.; Lindsley, C. W.; Stauffer, S. R.; Zhou, Y.; Macdonald, G.; Bartolome, J. M. Substituted-6-methylnicotinamides as mGluR5 positive allosteric modulators. WO2011149963, 2011.

(50) Conn, J. P.; Lindsley, C. W.; Weaver, C. D.; Stauffer, S.; Williams, R.; McDonald, G.; Bartolome-Nebreda, J. M.; Zhou, Y. Preparation of *O*-benzyl nicotinamide analogs as mGluR5 positive allosteric modulators. WO2011035324, 2011.

(51) Kubas, H.; Meyer, U.; Krueger, B.; Hechenberger, M.; Vanejevs, M.; Zemribo, R.; Kauss, V.; Ambartsumova, R.; Pyatkin, I.; Polosukhin, A. I.; Abel, U. Discovery, synthesis, and structure–activity relationships of 2-aminoquinazoline derivatives as a novel class of metabotropic glutamate receptor 5 negative allosteric modulators. *Bioorg. Med. Chem. Lett.* **2013**, *23*, 4493–4500.

(52) Liu, F.; Grauer, S.; Kelley, C.; Navarra, R.; Graf, R.; Zhang, G.; Atkinson, P. J.; Popielek, M.; Wantuch, C.; Khawaja, X.; Smith, D.; Olsen, M.; Kouranova, E.; Lai, M.; Pruthi, F.; Pulicicchio, C.; Day, M.; Gilbert, A.; Pausch, M. H.; Brandon, N. J.; Beyer, C. E.; Comery, T. A.; Logue, S.; Rosenzweig-Lipson, S.; Marquis, K. L. ADX-47273 [*S*-(4-fluoro-phenyl)-{3-[3-(4-fluoro-phenyl)-[1,2,4]-oxadiazol-5-yl]-piperidin-1-yl}-methanone]: a novel metabotropic glutamate receptor 5-selective positive allosteric modulator with preclinical antipsychotic-like and procognitive activities. *J. Pharmacol. Exp. Ther.* **2008**, *327*, 827–839.

(53) Lindsley, C. W.; Stauffer, S. R. Metabotropic glutamate receptor 5-positive allosteric modulators for the treatment of schizophrenia (2004–2012). *Pharm. Pat. Anal.* **2013**, *2*, 93–108.

(54) Rook, J. M.; Vinson, P. N.; Bridges, T. M.; Stauffer, S. R.; Ghoshal, A.; Daniels, J. S.; Niswender, C. M.; Lavreysen, H.; Mackie, C.; Bartolome, J. M.; Macdonald, G. J.; Steckler, T.; Jones, C. K.; Lindsley, C. W.; Conn, J. P. Discovery of Metabotropic Glutamate Receptor Subtype 5 PAMs that Display Stimulus Bias Reveals that in Vivo Efficacy in Animal Models can be Achieved Without Direct Potentiation of NMDAR Currents. Presented at ACNP 52nd Annual Meeting, Hollywood, FL, Dec. 8–12, 2013, Poster W203.

(55) Jain, A. N. Virtual screening in lead discovery and optimization. *Curr. Opin. Drug Discovery Dev.* **2004**, *7*, 396–403.

(56) Jain, A. N. Ligand-based structural hypotheses for virtual screening. *J. Med. Chem.* **2004**, *47*, 947–961.

(57) Rodriguez, A. L.; Nong, Y.; Sekaran, N. K.; Alagille, D.; Tamagnan, G. D.; Conn, P. J. A close structural analog of 2-methyl-6-(phenylethynyl)-pyridine acts as a neutral allosteric site ligand on metabotropic glutamate receptor subtype 5 and blocks the effects of multiple allosteric modulators. *Mol. Pharmacol.* **2005**, *68*, 1793–1802.

(58) Keseru, G. M.; Makara, G. M. The influence of lead discovery strategies on the properties of drug candidates. *Nature Rev. Drug Discovery* **2009**, *8*, 203–212.

(59) Shultz, M. D. The thermodynamic basis for the use of lipophilic efficiency (LipE) in enthalpic optimizations. *Bioorg. Med. Chem. Lett.* **2013**, *23*, 5992–6000.

(60) Gregory, K. J.; Noetzel, M. J.; Rook, J. M.; Vinson, P. N.; Stauffer, S. R.; Rodriguez, A. L.; Emmitte, K. A.; Zhou, Y.; Chun, A. C.; Felts, A. S.; Chauder, B. A.; Lindsley, C. W.; Niswender, C. M.; Conn, P. J. Investigating metabotropic glutamate receptor 5 allosteric modulator cooperativity, affinity, and agonism: enriching structure–function studies and structure–activity relationships. *Mol. Pharmacol.* **2012**, *82*, 860–875.

(61) Di, L.; Rong, H.; Feng, B. Demystifying brain penetration in central nervous system drug discovery. Miniperspective. *J. Med. Chem.* **2013**, *56*, 2–12.

(62) Niswender, C. M.; Johnson, K. A.; Luo, Q.; Ayala, J. E.; Kim, C.; Conn, P. J.; Weaver, C. D. A novel assay of Gi/o-linked G protein-coupled receptor coupling to potassium channels provides new insights into the pharmacology of the group III metabotropic glutamate receptors. *Mol. Pharmacol.* **2008**, *73*, 1213–1224.